https://doi.org/10.5194/egusphere-2026-4919
Preprint. Discussion started: 17 September 2026

Biome.jl v0.1.0: a modular platform for mechanistic biome modeling and hypothesis testing

Capucine Marie Sophie Lechartre[1], Victor Boussange[1], Dirk Nikolaus Karger[1], Jed Oliver Kaplan[2], Philipp Brun[1], Niklaus Emmanuel Zimmermann[1]

[1]Swiss Federal Research Inst. WSL, Birmensdorf, 8093, Switzerland.
[2]Department of Earth, Energy, and Environment, University of Calgary, Calgary, AB T2L 2A3, Canada

Correspondence to: Capucine M. S. Lechartre (capucine.lechartre@wsl.ch)

https://doi.org/10.5194/egusphere-2026-4919
Preprint. Discussion started: 17 September 2026

Abstract. Many global vegetation and biome models represent plant diversity through plant functional types (PFTs) and physiological processes. To map biomes, established models rely on fixed PFT definitions and established biome attribution schemes, which limit their adaptability to investigate new questions. Increased availability of high-resolution climate and species distribution datasets, as well as advanced computational power, now enable regional parameterization and conceptual extension of biome models, but this potential remains underutilized. Here, we present Biome.jl, a framework that unifies climate-based biome classification and mechanistic simulations of biological processes within a single, modular engine. The Biome.jl framework introduces a generalized dominance-based competition scheme in which the attribution of model pixels to a biome is determined by environmental suitability, potential productivity of PFTs, rules to translate PFTs to biomes, and biome dominance hierarchies. We evaluate Biome.jl against independent datasets, demonstrating that improved flexibility does not come at the cost of predictive power. We then illustrate the framework's customizability through two case studies: a regional parameterization of PFTs using multi-parametric grid search inference based on empirical data, and an extension of the base model with a novel stem succulent PFT and biome definition, achieved without modifying model components. By facilitating the comparison of biome concepts, offering flexible functional parameterization, and supporting multi-resolution implementation, Biome.jl redefines equilibrium biome modeling as a modular, hypothesis- and data-driven endeavor. It provides a foundation for testing climate-vegetation relationships and exploring uncertainty in biome projections under past, current, and future environmental conditions.

Short summary

Predicting how vegetation distribution responds to climate requires models that can be adapted to different regions and ecological questions. We present Biome.jl, a mechanistic modeling framework that allows customizing vegetation types, simulating their distribution, testing alternative biome concepts, and parameterizing the model using observational data. We demonstrate its capacity with case studies, predicting tree lines in the Swiss Alps and reproducing the global distribution of stem succulents.

https://doi.org/10.5194/egusphere-2026-4919
Preprint. Discussion started: 17 September 2026

1 Introduction

Understanding how vegetation responds to climate change is facilitated by biome models that link climate forcing to vegetation patterns through physiological processes. Since the introduction of the term "biome" in the early twentieth century (Clements, 1917), a wide range of modeling tools and classification schemes have been developed to map Earth's major vegetation zones (e.g., Box, 1995; Holt et al., 2013; Köppen, 1936; Olson et al., 2001; Fischer et al., 2022). These tools are particularly valuable for future vegetation projections and the study of climate-vegetation feedbacks across evolutionary timescales, which span centuries to millions of years. Yet, many current vegetation models were developed before high-resolution climatic datasets and globally consistent vegetation distribution maps became available, and their design usually limits their capacity to fully exploit the richness of the observational record that is now available (Wüest et al., 2020). Additionally, quantifying uncertainty in vegetation projections and testing how predictions depend on the chosen biome concept or the climate inputs used to force the model places new demands on existing frameworks. Meeting these demands requires tools that can flexibly represent competing biome concepts and vary the climatic inputs driving them within a single, unified platform, a combination that current models do not provide.

Climate is the primary factor driving plant ecological differentiation across space and time (Gonzalez et al., 2010; Kreft & Jetz, 2007; Woodward et al., 2004; Woodward & Williams, 1987), a relationship recognized since the early days of plant geography (Grisebach, 1872; Humboldt, 1806; Schimper, 1908). Different climatic and environmental conditions have led to the evolution of specific plant traits at the individual level and mediate dominance hierarchies among growth forms and species at the community level (Delcourt et al., 1982; Hordijk et al., 2025; Joswig et al., 2022). The current, unprecedented pace of climate change is expected to drive more than a third of the planet's surface toward novel ecosystems (Loarie et al., 2009; Ordonez et al., 2024) and poses significant challenges to all biota to track their spatially shifting ecological niches. Understanding these challenges by reliably simulating climate-vegetation interactions across a range of conditions, including non-analogous climates, demands novel and flexible model frameworks.

Because biome distributions have shifted repeatedly through evolutionary time, present-day biome patterns cannot be treated as fixed reflections of current climate alone (Mucina, 2019), and observed biomes may differ from climatic expectations even under stable conditions (Maiorano et al., 2013). Mechanistic biome models address this by simulating biome distribution through physiological, demographic, and ecosystem-level processes operating under climatic and edaphic constraints (Quillet et al., 2010). They represent vegetation as species-agnostic plant functional types (PFTs) rather than relying on species' realized distributions used by climate-envelope approaches (Champreux et al., 2024; Pilowsky et al., 2022; Smith et al., 1993). Since their introduction in vegetation modeling (Prentice et al., 1992; Smith & Huston, 1989; Smith et al., 1993; Solomon & Shugart, 1993), PFTs have become central to mechanistic approaches, encoding variation in growth form, phenology, and photosynthetic pathway when linking climate conditions to biome-level patterns (Anderegg et al., 2022; Box, 1995; Defries & Townshend, 1999).

https://doi.org/10.5194/egusphere-2026-4919
Preprint. Discussion started: 17 September 2026

Mechanistic vegetation models fall into two broad families: equilibrium models and dynamic global vegetation models (DGVMs). Equilibrium models (e.g., MAPSS, BIOME4) simulate the stable PFT configuration expected under a given climate (Kaplan, 2001; Neilson, 1995), while DGVMs (e.g., MC1, LPJ, CLM, ORCHIDEE) resolve high-frequency processes and feedbacks and are primarily designed for contemporary ecosystem dynamics rather than long-term or evolutionary questions (Bachelet et al., 2001; Fisher et al., 2015; Krinner et al., 2005; Lawrence et al., 2019; Li et al., 2024; B. Smith et al., 2014). The coarse temporal structure and computational efficiency of equilibrium models make them well-suited for global, high-resolution, long-term, and non-analogous climate contexts (Li et al., 2024) while still maintaining a high level of detail about vegetation structure.

However, the architecture of this type of model is often rigid. Most global models still represent terrestrial plant diversity with fewer than 20 (often only six) PFTs, oversimplifying important functional variation (Anderegg et al., 2022). Fixed PFT definitions and hard-coded rule sets prevent users from adjusting physiological thresholds to account for regional evolutionary histories (Gerber et al., 2004), from testing alternative functional classifications, or from extending models with novel PFTs where required. At the biome level, although numerous competing classification schemes exist (Beierkuhnlein & Fischer, 2021; Fischer et al., 2022; Whittaker, 1970), most mechanistic models implement only a single scheme for classifying PFT presence and productivity into biomes (Champreux et al., 2024), making it difficult to assess how the chosen conceptual framework influences predictions or to compare biome concepts under the same climatic forcing.

To help overcome these challenges, we developed Biome.jl, a flexible framework for mechanistic biome modeling that unifies climate-based biome classification and mechanistic process modeling within a single, modular engine. It is a platform designed for formulating, mapping, and comparing biome concepts under selected climate, soil, and CO_2 conditions. Biome.jl (1) runs at and scales to any spatial resolution, (2) supports parameter inference to parameterize PFT definitions against observational data, and (3) accommodates multiple biome classification schemes, which can be interchanged or compared without modifying the underlying physiological engine. By separating core processes (physiological filters, productivity, competition) from user-defined PFTs and biome attributions, Biome.jl provides a transparent platform to test hypotheses and generate data-driven predictions about climate-vegetation relationships. In this paper, we describe the structure and assumptions of Biome.jl, explain how it was parameterized and validated, and explore its performance across two case studies.

2 Methods

2.1 Framework overview

https://doi.org/10.5194/egusphere-2026-4919
Preprint. Discussion started: 17 September 2026

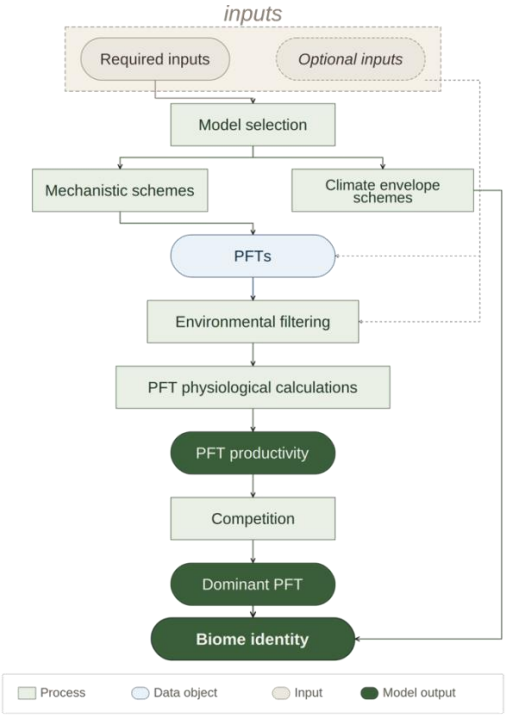

Figure 1. Biome.jl architecture. Rectangles represent model choices and processes, and capsules represent simulated objects. Dark green objects represent model outputs. *PFT* stands for plant functional type, which is represented in blue, as a data object, which holds parameters. The schematic illustrates the mechanistic simulation pathway in Biome.jl for a set of PFTs given climate and soil variables. This core spans environmental filtering of adapted PFTs, productivity estimation, competition outcomes, and the generation of output variables.

The model can (1) run climate-envelope schemes to generate biome maps based on established climatic niches (Fig. 1). These include the commonly used classifications of Köppen-Geiger (Köppen, 1936), Wissmann (Wissmann, 1939), Thornthwaite (Thornthwaite, 1931, 1948), and Troll-Paffen (Troll & Paffen, 1964). It can also (2) perform mechanistic simulations at the PFT level using the widely used BIOME4 model or a user-defined modification of this model that shares its core assumptions. The main output is a biome map in all cases, but mechanistic simulations additionally provide PFT-level productivity and the dominant biome vegetation within each grid cell (Fig. 1). In the mechanistic case, biome distributions are assumed to depend on climate, soil, and CO_2 constraints: the engine simulates the distribution of a set of PFTs, their net primary productivity (NPP), and competition amongst them. It then uses these variables to predict biomes over a region of interest. In the model, the abiotic environment is represented by a set of environmental input variables and internally computed characteristics. The PFTs and their competitive interactions represent the biotic environment.

Biome.jl operates on a gridded landscape and simulates equilibrium conditions. At equilibrium, a neighboring cell's identity is independent of the focal pixel's type, including at ecotones, which are transition zones between biomes.

https://doi.org/10.5194/egusphere-2026-4919
Preprint. Discussion started: 17 September 2026

This allows pixels to be processed in parallel to optimize runtime. The resolution of the Biome.jl outputs therefore solely depends on the resolution of the input dataset.

The modeling framework is openly available to the research community as a software package and written in the Julia language (Bezanson et al., 2012). An R-language wrapper, named biomeR, is available to safeguard the benefits of Julia while allowing its execution in R (R Core Team, 2025), a language mostly used by ecologists and Earth systems scientists. Both are made available on GitHub to promote community-driven development. Below, we explain the Biome.jl inputs, its parameterization, configurations, and the different simulation modes.

2. 2 Model inputs

2.2.1 Environmental data

The Biome.jl framework is designed to run using gridded climatologies, typically 30-year monthly or daily averages of the variable of interest, imported as Rasters.jl objects. Environmental input is expected to be provided by grids of identical scale, alignment, and projection, as the engine works pixel-wise on stacked environmental input. At a minimum, Biome.jl expects information on climatological monthly mean temperature and total precipitation. These inputs are sufficient to run simulations with all available climate-envelope schemes in the modeling framework. For the mechanistic schemes, additional climate and soil rasters are required as inputs, along with a single global atmospheric CO_2 concentration (Table 1). Several climatic indices used by the mechanistic models are derived internally from these inputs unless explicitly provided by the user (Table 1). A useful resource for approximating the soil variables required in the mechanistic schemes is the makesoil repository from ARVE Research, available at https://github.com/ARVE-Research/makesoil.git. It uses SoilGrids soil properties (Poggio et al., 2021) and pedotransfer functions to estimate the soil hydraulic properties of water holding capacity and saturated conductivity.

Additional optional inputs can be passed to the model if they are provided on the same grid. They can help delineate user-defined niche limits of PFTs by introducing additional physiological constraints. They can also replace internal calculations with observational data, for example, by replacing the interpolation of daily variables from monthly values. The internally calculated climatic variables that can be overwritten are presented in Table 1 as mechanistic optional variables (Table 1). Careful comparison of additional inputs to internally calculated variables should be performed ahead of productive model runs to ensure that the model remains physically consistent. Additional constraints may be introduced for any variable, provided they are also supplied as inputs with corresponding units. For example, vapor pressure deficit, usually expressed in Pa, could be added as a constraint, as it is known to increase the risk of hydraulic failure and potentially limits the establishment of species (Grossiord et al., 2020).

Table 1: Required inputs and derived climate variables, which can be provided as optional inputs used by the Biome.jl engine and its outputs. Only air temperature and precipitation rates are required in all schemes, while the additional variables cloud cover, soil saturated conductivity, soil water holding capacity, and CO_2 are required in the mechanistic schemes (Fig. 1, Mechanistic required). Mechanistic optional variables can be supplied as additional inputs, which

https://doi.org/10.5194/egusphere-2026-4919
Preprint. Discussion started: 17 September 2026

automatically override model calculations for that variable, without changes to the code. Any other additional input variables would not override internal computations and are therefore not listed here. All time-relative resolution is expected to be provided as a climatological average.

Variable	Abbreviation	Unit	Frequency	Description
Inputs				
All schemes				
Monthly temperature	tas	°C	monthly	monthly mean near-surface (2 m) air temperature
Monthly precipitation	pr	kg m^{-2} $month^{-1}$	monthly	precipitation rate
Mechanistic required				
Total Cloud Cover Percentage	clt	%	monthly	monthly mean cloudiness
Water holding capacity	whc	kg m^{-2} $month^{-1}$ $layer^{-1}$	depth level	plant-available water storage capacity
Soil saturated conductivity	ksat	kg m^{-2} h^{-1} $layer^{-1}$	depth level	effective saturated conductivity/percolation parameter.
CO_2	co2	ppm	single value	single global atmospheric value of carbon dioxide
Mechanistic optional				
Daily temperature	dtas	°C	daily	daily mean near-surface (2 m) air temperature
Daily precipitation	dpr	kg m^{-2} day^{-1}	daily	daily precipitation rate
Daily cloud cover	dclou	%	daily	daily average cloud cover
Snow melt	dmelt	kg m^{-2} day^{-1}	daily	meltwater released from snowpack
Potential evapotranspiration	dpet	kg m^{-2} day^{-1}	daily	combined loss of water through plant transpiration and soil surface evaporation
Daily day length	ddayl	hours	daily	daily illumination hours
Monthly day length	dayl	hours	monthly	mid-month daily illumination hours
Solar radiation	sun	J m^{-2} day^{-1}	monthly	total incoming shortwave radiation for a representative day of the month
Absolute minimum temperature	tmin	°C	single value	minimal temperature reached within a climatological year
Solar radiation	rad0	GJ m^{-2} yr^{-1}	single value	total annual photosynthetically active radiation (PAR) accumulated over months with mean temperature > 0 °C
Temperature of the coldest month	tcm	°C	single value	coldest temperature in monthly averages
Temperature of the warmest month	twm	°C	single value	warmest temperature in monthly averages
Growing degree days above 0°C	gdd0	°C day^{-1}	single value	cumulated daily degrees above a 0 °C temperature threshold
Growing degree days above 5°C	gdd5	°C day^{-1}	single value	cumulated daily degrees above a 5 °C temperature threshold
Total precipitation	tpr	kg m^{-2} $year^{-1}$	single value	annual precipitation rate

https://doi.org/10.5194/egusphere-2026-4919
Preprint. Discussion started: 17 September 2026

Maximum snow depth	maxdepth	cm	single value	maximum snowpack depth accumulated over the year
Outputs				
All schemes				
Biome classification	koppen_class, thornthwaite_temperature_zone and thornthwaite_moisture_zone, troll_zone, wissmann_climate_zone, biome		single value	biome classification according to the chosen scheme
Mechanistic schemes				
Dominant PFT	optpft		single value	Most competitive PFT in the pixel cell
NPP	npp	g C m^{-2} yr^{-1}	per PFT	Expected PFT-level productivity

2.2.2 Configurations

In addition to environmental data, mechanistic simulation schemes require a specification of PFTs, their associated parameterization, and a mapping of PFTs to biome classes. These inputs are ignored by climate-envelope schemes. Within Biome.jl, the BIOME4 configuration is available, including the original PFTs (Kaplan, 2001) and a PFT-to-biome mapping. Alternatively, users may supply custom PFT definitions and biome translation schemes when using the customizable base, presented later. These custom configurations are intended to support more or less granular or alternative biome concepts. Users configure simulations through a model setup orchestrator, which combines the supplied inputs with the chosen climatic or mechanistic scheme. We provide users with a comprehensive tutorial for model customization in the package documentation.

2.3 Model outputs

The different modeling approaches produce distinct types of outputs. All schemes return a Rasters.jl object that can be saved into a NetCDF file with explicit X/Y-coordinates taken from the input grids and their projections. Uniform outputs allow climatic and mechanistic outputs to be compared on the same grid as the input variables. Climatic schemes return single-layer categorical biome maps, with each grid cell assigned an integer class representing the biome according to the selected conceptual classification. Mechanistic schemes also produce a categorical biome map derived from the specified PFT-to-biome translation scheme. They also return layers of net primary productivity (NPP) in g C m^{-2} yr^{-1} for each PFT, and of the dominant PFT per grid cell (Table 1). For all provided schemes, the correspondence between integer values and biome classes is provided through a class key in the model documentation, ensuring that map legends are unambiguous and reproducible (see Fig A1 for an example of biome classification maps and legends).

https://doi.org/10.5194/egusphere-2026-4919
Preprint. Discussion started: 17 September 2026

2.4 Climate envelope schemes

The climate-envelope schemes were reimplemented in Julia by directly transcribing the classification logic from the SAGA-GIS tool Climate Classification (Conrad et al., 2015).They provide a basic climate zone classification based on minimal climatological input and are thus applicable in many contexts and are rapidly calculated. They have no mechanistic basis or explicit link to PFTs or dominant plant traits (see below)

Köppen-Geiger: The Köppen-Geiger scheme groups climate into five major categories (A-E) based on thresholds for monthly temperature and precipitation, as well as the seasonal timing of wet and dry periods (Köppen, 1936, Kottek et al., 2006). Its logic is vegetation-driven without explicitly assigning PFTs or dominant plant traits to the final classes. This scheme relies on the premise that, generally, monthly means and seasonal contrasts better capture ecological constraints than annual averages (Fig. A1a).

Thornthwaite: The Thornthwaite system classifies climates based on how well precipitation meets evaporative demand and on the overall thermal energy available (Thornthwaite, 1931, 1948). Using monthly temperature and precipitation, it assigns every location to one of five moisture zones and six temperature zones. Its structure links moisture balance and heat availability to ecological potentials (Fig. A1b), partly assigning dominant plant traits to the resulting classes.

Troll-Paffen: The Troll-Paffen classification defines 38 climate types by examining how three seasonal regimes: radiation, temperature, and moisture interact through the year (Troll & Paffen, 1964). It captures the interference between “seasonal climates” in temperature and precipitation to distinguish patterns from polar ice deserts to tropical rainforests (Troll & Paffen, 1964) (Fig. A1c), thus assigning dominant PFTs or plant traits to the resulting classes.

Wissmann: The Wissmann scheme organizes global climates into six broad thermal groups, then differentiates them using moisture thresholds that separate rainforest, monsoonal, steppe, and desert environments (Wissmann, 1939). It considers summarized monthly temperature and precipitation values and uses a dynamic precipitation limit that is linearly related to mean annual temperature and adjusted depending on whether summer or winter is wetter. This approach directly ties climatic moisture availability to thermal conditions and the seasonality of climatic conditions (Fig. A1d) and implicitly assigns classical biomes to the resulting classes.

2.5 Mechanistic schemes

The mechanistic engine of Biome.jl is built around a customizable physiological core derived from the BIOME4 model (Haxeltine & Prentice, 1996; Kaplan, 2001), which handles environmental filtering, productivity estimation, and the representation physiological limits to PFTs (Fig. 1). The primary contribution of Biome.jl is a generalized and fully customizable mechanistic framework, hereafter referred to as the "customizable base", which builds on the physiological computation routines of BIOME4 but allows users to define new PFTs, modify the competition logic, and specify flexible PFT-to-biome mapping schemes. To ensure continuity with the existing literature and enable direct benchmarking, Biome.jl additionally provides a reference implementation of the original BIOME4 model that retains its original logic without modification (Fig. A1.e). The two schemes share the same representation of

https://doi.org/10.5194/egusphere-2026-4919
Preprint. Discussion started: 17 September 2026

physiological processes and differ only in how competition among PFTs is formulated and how dominant PFTs are attributed to biome classes. The shared components are described in Sect. 2.5.1–2.5.3; departures specific to the customizable base are noted explicitly where they occur.

Customizable base: The customizable base inherits the BIOME4 physiological routines for computing PFT growth and productivity but replaces the fixed competition logic and biome translation framework with a generalized, user-configurable alternative. It accepts any PFT definition within the required set of parameters and provided constraints and allows flexible PFT-to-biome mapping based on user-defined rules, making it Biome.jl's primary interface for hypothesis testing or regional parameterization. This mode is initialized with six PFTs intended to represent a basis for differentiation into more specific types (Fig. 2); it can accept new PFT definitions as well as the original BIOME4 PFTs, with or without modification.

BIOME4: Building on previous versions of BIOME models, the model simulates daily canopy conductance, photosynthesis, respiration, hydrology, phenology, and fire days for 13 PFTs (Kaplan, 2001). It then calculates the maximum leaf area index (LAI) and net primary productivity (NPP) that each PFT can sustain, given the local environmental conditions. Next, it uses these estimates to simulate competition among the co-occurring PFTs. Finally, based on the dominant PFTs within the cell, the model derives the pixel's potential biome identity (Kaplan, 2001). In Biome.jl, this scheme is implemented without modification to reproduce the behavior and outputs of the original BIOME4 model (Fig. A1.e). The following mechanistic components are shared by both the BIOME4 scheme and the customizable base, unless stated otherwise.

2.5.1 Defining PFTs

Each PFT is initialized with a list of 17 parameters (Table A1) influencing three main processes: photosynthesis, evapotranspiration, and root distribution. Biome.jl provides maximum flexibility in PFT definitions across all its mechanistic models: all parameters of individual PFTs can be adjusted through helper functions provided by the package, and new PFTs with user-defined parameters can be created. In the customizable base of Biome.jl, two parameters were added: the dominance class value D, which represents the PFT's potential dominance rank within its range, and the minimum sustainable LAI for the PFT to survive, both of which are defined in the original instances of the BIOME model (Box, 1995; Prentice et al., 1992). PFTs with low dominance class values (e.g., one, indicating the highest dominance rank) can dominate even at the edge of their ecological range, as is the case for tropical evergreen forest types, which dominate across their ecological gradient. PFTs with high values (e.g., eight, indicating a low dominance rank), such as cold herbaceous types, might be easily outcompeted even at the center of their niche if PFTs with higher dominance potential are present; their physiological potential is usually broader, but their ecological dominance is usually restricted to narrower climatic domains where conditions exclude more competitive PFTs.

Individual PFTs are additionally initialized with physiological constraints that delineate their fundamental ecological niche (Hallgren & Pitman, 2000; Haxeltine & Prentice, 1996). Constraints are defined based on variables derived

https://doi.org/10.5194/egusphere-2026-4919
Preprint. Discussion started: 17 September 2026

internally from the model inputs, including upper and lower climatic limits for the warmest and coldest months, absolute minimum temperature tolerance, growing degree days at 5 °C and 0 °C, snow depth (Table S1). The customizable base optionally takes site water balance as an additional constraint, expressed as a percentage of field capacity (see Sect. 2.5.2). As mentioned above, additional constraints of the fundamental niche can be parameterized for PFTs, provided the corresponding environmental variable is supplied as input. Ecophysiological thresholds can be derived from the literature or inferred from species or PFT observations (Beigaitė et al., 2022).

2.5.2 Environmental filtering of PFTs

The engine applies bioclimatic limits by comparing each PFT's physiological constraint thresholds against the grid cell's computed climatological characteristics (Kaplan, 2001). To limit assumptions about the fundamental distribution of each PFT, not all PFTs are defined with all possible limits; only the most representative ones can be specified, while the tolerance limits that are not relevant to the PFT distribution can remain undefined. Each defined environmental variable has its own PFT-specific minimum and/or maximum tolerated values, and a PFT is viable only if all its thresholds are satisfied independently.

Soil moisture is not used as a constraint to PFT growth in BIOME4. Because it strongly limits tree growth (Harrison & Prentice, 2003), the customizable base model applies an additional filtering step based on comparing potential water availability to each PFT's evapotranspirative demand. This limits PFT growth according to their humidity constraints and removes them from the pool of potentially present PFTs if the constraints are exceeded. In the model, soil moisture available to each PFT is derived from the site water balance calculation developed in earlier BIOME models (Haxeltine & Prentice, 1996; Kaplan et al., 2003). It is a variable that depends on soil parameters and climate, and has been proven to correlate with PFT distribution (Brun et al., 2022; Neilson, 1995; Woodward, 1987). Site water balance is driven by daily equilibrium evapotranspiration (Prentice et al., 1993), where equilibrium evapotranspiration is obtained from latitude, temperature, and cloud cover via the net-radiation balance. Actual evapotranspiration is then scaled from this equilibrium demand and limited by root-zone supply. Adding daily precipitation and snowmelt allows calculation of the water content of upper and lower soil layers while considering the effects of percolation, drainage, and runoff. We then extract, for each month, the mean water content of the upper soil layer expressed as a percentage of field capacity (0–100 %) and average these twelve monthly values into a single annual soil-moisture value per PFT. This value is compared against each PFT's site water balance constraint, and as for other constraints, a PFT is considered potentially present only if the pixel value falls within these bounds and is otherwise removed. Finally, the model imposes an LAI screen: for each pixel, the PFT's LAI is computed and, if it falls below the PFT's minimum sustainable threshold (Haxeltine & Prentice, 1996, Table 5), it is discarded from the candidate pool. As previously noted, users can provide additional environmental variables as inputs to refine fundamental niche constraints to PFTs.

https://doi.org/10.5194/egusphere-2026-4919
Preprint. Discussion started: 17 September 2026

2.5.3 Dominance-based competition for assigning biomes

Competition is handled differently in the BIOME4 scheme and in the customizable base, reflecting their distinct assumptions about PFT definition and biome attribution. The competition frameworks defined in the BIOME3 and BIOME4 model versions identify dominance by comparing the NPP of predefined grass and woody PFTs to determine the single dominant PFT (Haxeltine & Prentice, 1996; Kaplan, 2001), then apply a complex set of relationships that simulate inter-PFT competition and partly override the NPP-defined dominance. In the customizable base of Biome.jl, the competition logic accommodates a flexible PFT definition. It simplifies the competitive relationships and does not depend on known relationships between pre-defined PFTs. The estimates of competitive ability are calculated from each PFT's environmental suitability in a climatic envelope defined by its fundamental niche dimensions, its potential NPP, and the dominance parameter. All PFTs present in the evaluated cell are ranked based on this competitive score, and the PFT with the highest value is chosen as the dominant PFT (see Appendix B for a detailed description of the calculations).

2.5.4 Parameterization

Unlike legacy BIOME4 implementations in which physiological parameters are hard-coded in compiled Fortran and cannot be modified without rewriting the source, Biome.jl exposes all PFT parameters as native Julia variables. This makes the model directly compatible with inference approaches without requiring wrappers or custom gradient definitions. Given the low dimensionality of the parameter space and the Julia implementation's computational efficiency, grid search-based sampling can be performed across multiple parameters simultaneously. Exposing PFT parameters directly allows new PFTs to be parameterized against observational data. Given that no globally agreed PFT scheme currently exists, and therefore there are no definitive PFT distribution or trait maps (Harrison et al., 2010), parameterization allows for formulating and validating new PFT definitions (see Case study 2). Parameterization further allows PFTs to be tuned regionally: although the aggregation of taxa into PFTs assumes generalizable environmental responses (Smith et al., 1993), regional tuning makes it possible to address specific research questions without resorting to species-level modeling. An example of the parameterization workflow used in Case study 1 is available in the package's GitHub repository (see Code and Data availability).

The original BIOME4 PFTs (Kaplan, 2001) are included with default configurations but can also be modified and used in the customizable base. The PFTs of the customizable base are intended to be modified by users depending on their research interest; the simple starting set includes a needleleaf evergreen, a broadleaf evergreen, a needleleaf deciduous, a broadleaf deciduous type, a C3 and a C4 grass type. Their physiological constraints were estimated from simulated maps of forest types derived from empirical inventory data as binary response variables (Ma et al., 2023) and matched to the distribution of model variables (Fig. 2).

https://doi.org/10.5194/egusphere-2026-4919
Preprint. Discussion started: 17 September 2026

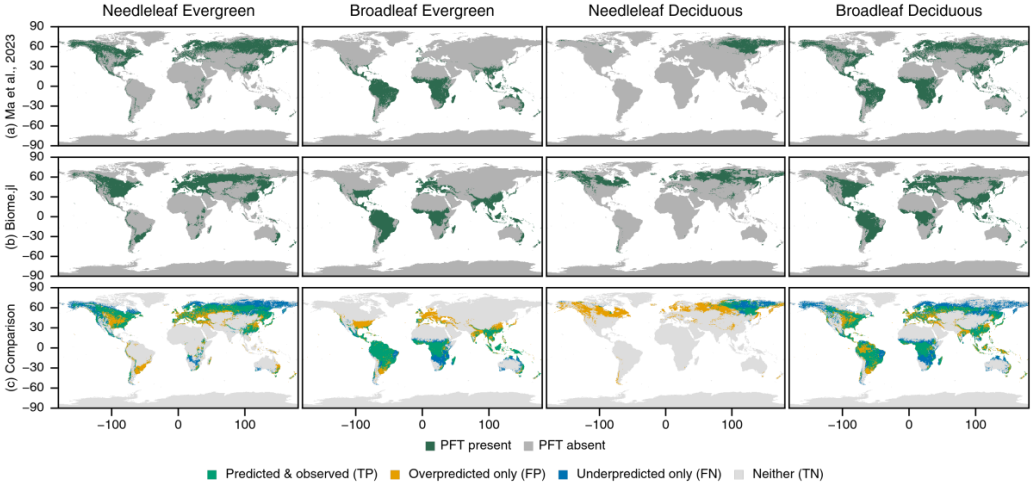

Figure 2. (a) Reference maps from Ma et al. (2023) of the distribution of the tree PFTs provided in the customizable base of the engine. (b) Modeled distribution of the PFT according to Biome.jl and the distributional constraints as estimated from the upper panel maps. (c) Comparison between the Ma et al. (2023) simulated maps and the maps computed with the customizable base. Colors highlight: in green, the agreement between the two maps (TP, true positives); in orange and blue, overprediction (FP, false positives) and underprediction (FN, false negatives), respectively. Gray represents true negatives (TN), where the PFT is never predicted.

2.6 Evaluation

Modifying the competition logic was necessary to allow the model to work with any new PFT. As we previously noted, several biome classifications exist, and their implementation differs across available datasets, making them difficult to rationalize and to evaluate. We compared the original BIOME4 competition scheme against the new dominance-based subroutine implemented in Biome.jl over broad vegetation categories that can be differentiated from satellite products (Aziz et al., 2024; Bai et al., 2023; Ma et al., 2023) using two reference datasets: the RESOLVE ecoregions dataset (Dinerstein et al., 2017), which is based on based on the widely employed 2001 Ecoregion concept (Olson et al., 2001), and the Global Land Cover by National Mapping Organizations (GLCNMO) raster (Kobayashi et al., 2017), a MODIS-based land cover classification dataset. We selected these two datasets because they complement each other along the axis of potential versus observed vegetation. RESOLVE represents potential natural vegetation consistent with the target of our biome models, and provides globally smooth coverage. GLCNMO is derived from satellite products and thus reflects observed vegetation but includes land-use classes whose pixels cannot be compared to our modeling outputs. We aggregated RESOLVE ecoregions across two classification levels: (1) a coarse tree vs. grass distinction, and (2) six broad biome types (tropical forest, temperate and boreal forest, savanna and tropical grassland, temperate grassland and shrubland, tundra, and desert). We also aggregated the GLCNMO dataset into (1) a coarse tree vs. grass distinction, and (2) broad biome types (broadleaf evergreen, broadleaf deciduous, needleleaf evergreen, needleleaf deciduous, mixed forest, grass). Analyses were conducted at the global scale with 0.5° resolution and at the continental scale (Europe) with 30 arc-second resolution (30”, about 1 km at the equator).

https://doi.org/10.5194/egusphere-2026-4919
Preprint. Discussion started: 17 September 2026

Results were evaluated using micro-averaged and per-class F1 scores, which represent the harmonic mean of the model's precision and recall, computed from contingency matrices. Because some biome types were not represented in the evaluation datasets over the European landscape (i.e., broadleaf evergreen, savanna and tropical grassland, and tropical forest), they were not tested at 30" (Table 2).

The climate-based schemes implemented in Biome.jl have been previously evaluated against observational and benchmark datasets and extensively employed across studies (e.g., Ahti et al., 1968; Cui et al., 2020; Marti et al., 2023; Navarro et al., 2025; Köppen-Geiger concept: Beck et al., 2023; Klinges et al., 2025.; Willmes et al., 2017, Thornthwaite concept: Whittaker, 1956, Troll-Paffen concept: Portmann et al., 2010, Wissmann concept: Ohsawa, 1991). Additionally, the BIOME4 model has been evaluated against multiple observational and benchmark datasets (e.g., Harrison & Prentice, 2003; Kaplan et al., 2003; Salzmann et al., 2008; Wanner et al., 2008). Consequently, we focused on evaluating the impact of the newly introduced competition subroutine on prediction accuracy rather than reassessing the climatic inputs or the core BIOME4 formulation.

Table 2. MicroF1 and F-Score per vegetation class for a 0.5° global and 30" regional (Europe) comparison of the two competition schemes, BIOME4, the original model logic, and BIOME4 with the new dominance-based competition, with the GLCNMO and RESOLVE bioregion datasets.

				0.5° global		30″ continental	
Ground truth	**Grouping**	**Class**	**Metric**	**BIOME4 with Dominance based competition**	**BIOME4**	**BIOME4 with Dominance based competition**	**BIOME4**
GLCNMO	**Tree/Grass**		*microF1*	**0.90**	0.89	0.72	**0.73**
		Tree	*Per-class F1*	**0.69**	0.68	0.66	**0.68**
		Grass/shrub		**0.48**	0.39	0.28	0.28
	Forest types		*microF1*	**0.90**	0.89	**0.72**	0.69
		Broadleaf evergreen	*Per-class F1*	0.59	0.59	*Not tested*	*Not tested*
		Broadleaf deciduous		**0.18**	0.17	0.14	0.13
		Needleleaf evergreen		**0.18**	0.13	**0.35**	0.29
		Needleleaf deciduous		0.16	**0.26**	**0.04**	0.02
		Mixed forest		0.14	**0.19**	0.24	**0.25**
RESOLVE	**Tree/Grass**		*microF1*	0.80	0.80	0.89	**0.90**
		Tree	*Per-class F1*	0.75	0.75	0.87	**0.90**
		Grass/Shrub		0.33	**0.37**	0.65	**0.67**
	Biome types		*microF1*	**0.66**	0.64	0.74	**0.80**
		Temperate/Broadleaf forest	*Per-class F1*	0.73	**0.77**	0.88	**0.91**

https://doi.org/10.5194/egusphere-2026-4919
Preprint. Discussion started: 17 September 2026

Ground truth	Grouping	Class	Metric	0.5° global		30″ continental	
				BIOME4 with Dominance based competition	**BIOME4**	**BIOME4 with Dominance based competition**	**BIOME4**
		Temperate grassland and shrubland		**0.31**	0.30	0.52	**0.55**
		Savanna and tropical grassland		**0.52**	0.42	*Not tested*	*Not tested*
		Tropical forest		**0.72**	0.71	*Not tested*	*Not tested*
		Desert		0.72	**0.73**	0.09	**0.28**
		Tundra		**0.75**	0.64	0.28	**0.29**

Results were similar between the two competition schemes (Table 2, Fig. A2). Both achieved high Micro-F1 scores for the tree-grass distinction (GLCNMO: 0.90-0.89 globally, 0.72-0.73 regionally; RESOLVE: 0.80 globally, 0.89-0.90 regionally), with the dominance-based scheme performing comparably or slightly below or above BIOME4 for grass/shrub classification depending on the evaluation dataset. For the finer classifications, the dominance-based scheme matched or marginally exceeded BIOME4 at 0.5° against both references (RESOLVE biome types, Micro-F1: 0.66 vs. 0.64; GLCNMO forest types: 0.90 vs. 0.89), with per-class gains for grass/shrub (F = 0.48 vs. 0.39) and needleleaf evergreen forests (F = 0.18 vs. 0.13) under GLCNMO. At 30”, the two references diverged: BIOME4 matched more closely RESOLVE ecoregions (Micro-F1: 0.80 vs. 0.74), whereas the dominance-based scheme performed comparably or better against GLCNMO, for forest types overall (0.72 vs. 0.69) and for needleleaf evergreen forests (F = 0.35 vs. 0.29). Both models struggled most with grasslands and shrublands, consistent with known challenges in classifying transition zones (Haxeltine & Prentice, 1996; Kaplan, 2001), and performed poorly in desert and tundra at 30”, likely due to their low representation in the European domain. The two comparisons are complementary. Continental European plains are strongly affected by land use and poorly represented in the GLCNMO raster. However, mountainous regions, less modified by human activity, are better resolved by GLCNMO at this resolution, allowing altitudinal vegetation gradients and overall model performance to be evaluated more reliably (Fig. A2).

These results demonstrate that generalizing the competition logic by defining competitive ability based on environmental suitability, potential NPP, and dominance class does not degrade performance while allowing greater flexibility, at least for distinguishing broad biome classes. This confirms that the new scheme is a biologically coherent and ecologically relevant alternative for the PFT-specific competition rules of BIOME4, which were originally manually tuned to a specific input dataset and do not generalize to new PFTs or alternative climate or soil input fields. The differences in outputs between the original BIOME4 framework and the dominance-based competition subroutine, tested both using BIOME4 PFTs, are shown in panels (e) and (f) of Fig. A1.

https://doi.org/10.5194/egusphere-2026-4919
Preprint. Discussion started: 17 September 2026

3 Case studies

We present two case studies to highlight the potential applications of Biome.jl and the features of our package. The first case study illustrates the flexibility of Biome.jl in implementing mechanistic biome predictions at the regional scale, showcasing high-resolution outputs and parameter tuning to treeline vegetation. The second case study illustrates how Biome.jl can be extended to new PFTs and biome concepts and possible research outcomes. Both case studies are evaluated against modeling and observational data, underscoring the practical relevance of the modeling framework.

3.1 Case study 1. Treeline simulation in the Swiss Alps at 90 m resolution

In this first example, we use Biome.jl to simulate the climate-driven treeline position at the regional scale based on 30-year averages from 1981 to 2010 in the Swiss Alps. We use the forest mixture proportion data sampled at 90 m resolution from the Swiss National Forest Inventory (NFI) (Fischer & Traub, 2019) as a ground-truth dataset for estimating the physiological parameters influencing treeline position. We parameterize boreal evergreen and boreal deciduous PFTs across Switzerland using the CHELSA climatologies of temperature, precipitation, and cloud cover from 1981 to 2010 at a 90 m resolution (Zilker & Karger, 2025). While the position of the treeline in the Swiss Alps is highly influenced by land use (Gehrig-Fasel et al., 2007), the primary natural limit to treeline expansion at high elevation is temperature (Körner & Paulsen, 2004), and it is hypothesized that the treeline is mediated by the tree's annual growth and respiration requirements (Cooper, 1975; Prentice et al., 1992). We therefore focus on the model's primary temperature constraint on PFT growth, represented by growing degree days, the cumulative daily temperature excess above a 5 °C base threshold for trees (Prentice et al., 1992). Although BIOME4 also conditions PFT establishment on the mean temperature of the coldest month (T_{CM}) and the absolute minimum temperature (T_{min}), these constraints are not calibrated here. In the Swiss Alps, the cold-season temperature signal is strongly collinear with the growing-season signal along the elevation gradient used for parameterization, making their individual contributions non-identifiable from a single regional dataset. We therefore calibrate only the GDD_5 bounds, retaining T_{CM} and T_{min} at their BIOME4 default values, since exceeding thresholds in a single variable is sufficient to exclude a PFT from a pixel. Additionally, in alpine treeline conditions, establishment failure is driven by the minimum length of the growing season rather than by an upper warm-season constraint. We therefore only estimate the lower bound of the GDD_5 parameter, $GDD_{5,low}$.

We estimated $GDD_{5,low}$ via a grid search over 100 values spanning [100, 1800] degree-days, with a search resolution of approximately 17 degree-days that sets a lower bound on the precision of reported confidence intervals. At each grid point, BIOME4 was evaluated over an elevation-stratified subsample of pixels drawn from the NFI ground truth. We evaluated model fit using a soft binary log-likelihood, assigning log(0.85) to each pixel if its predicted, originally binary, presence or absence matched the observed ground truth, and log(0.15) otherwise. This assigns a fixed 85 % reliability to BIOME4's deterministic classification, converting the discrete presence/absence match into a Bernoulli likelihood suitable for confidence-interval estimation. We identified the maximum-likelihood estimate as the grid

https://doi.org/10.5194/egusphere-2026-4919
Preprint. Discussion started: 17 September 2026

point maximizing the resulting log-likelihood surface L($GDD_{5,low}$), and we derived 95 % profile confidence intervals. $GDD_{5,low}$ estimations converged into a well-resolved peak for both relevant PFTs (Fig. 3). We therefore calibrate $GDD_{5,low}$to rounded values of 443 degree-days (95 % CI below the grid search resolution) for boreal evergreen and 873 degree-days (95 % CI: [856, 890]) for boreal deciduous trees.

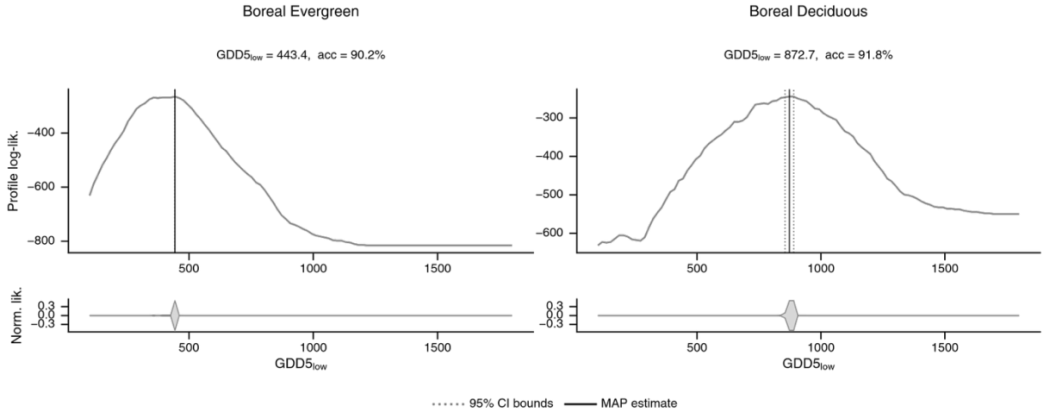

Figure 3. Results of parameter estimation using a grid search approach for GDD_5 parameters as profile log likelihood (Profile log. lik.) and normalized likelihood (Norm. lik.) for the lower bound of the GDD_5 limits, $GDD_{5,low}$ for boreal evergreen trees and boreal deciduous trees. Vertical bars indicate the selected parameter value, where MAP stands for maximum a posteriori estimate, the parameter value that maximizes the posterior distribution, and its 95 % confidence interval. Acc stands for accuracy, the fraction of sampled pixels whose predicted presence/absence matched the ground truth at the MAP parameter value.

We then ran Biome.jl on 90 m resolution climate data (Zilker & Karger, 2025), between longitudes 9.0 and 9.5 and latitudes 46.5 to 47.0 for the period 1980–2010, using the BIOME4 configuration with the new parameterization, and compared it with results from the globally parameterized mode, which we refer to as unparameterized in the following analysis. To do so, we aggregated relevant BIOME4 biome classes into below- and above-treeline categories.

We evaluated modeled treeline positions (1981–2010) against Copernicus Tree Cover Density (2012) (*Tree Cover Density 2012 (Raster 20m), Europe, 3-Yearly, Mar. 2018*, n.d.), masking pixels with < 70 % cover to define the reference treeline as forest-nonforest boundaries. Then, we applied a moving-window approach (20 x 20 pixels, stride 8) to the boundary, selecting within each window the highest-elevation boundary pixel above 1600 m. This produced a point-based treeline proxy that excluded most human influence. We compared modeled treeline masks to the horizontally nearest observation-based treeline proxy point. For each match, we computed vertical distances between modeled and proxy point based on the SRTM elevation raster at 90 m resolution (NASA JPL, 2013).

https://doi.org/10.5194/egusphere-2026-4919
Preprint. Discussion started: 17 September 2026

3.1.1 Results

Regarding treeline position, the regionally parameterized model predicted a mean treeline elevation of 1857 m against 2175 m for its unparameterized version (Fig. 4). When we computed the vertical difference between the modeled and the horizontally nearest treeline proxy points: the parameterized model showed negligible vertical bias (+ 22 m), with points distributed almost symmetrically above and below the proxy (57 % above), whereas the unparameterized model predicted systematically higher (bias + 228 m; 95 % of points above). Because the selected highest treeline points approximate the realized treeline and might remain affected by land use (Gehrig-Fasel et al., 2007), the parameterized model is in close agreement with the observed forest limit, while the large positive bias of the unparameterized model is consistent with the original BIOME4 parameterization approximating the potential climatic treeline at a global scale (Körner & Paulsen, 2004). Regional parameterization in Biome.jl improves agreement with the observed treeline without altering core model structure. This step makes the framework scalable to regional mechanistic mapping and readily transferable to new regions or mountain systems. We estimate that further considering slope, aspect, and soil characteristics would complement downscaled climatic data in accurately representing the heterogeneous terrain of the Swiss Alps. Those methodological developments would improve the model's ability to resolve biome boundaries at very high resolutions.

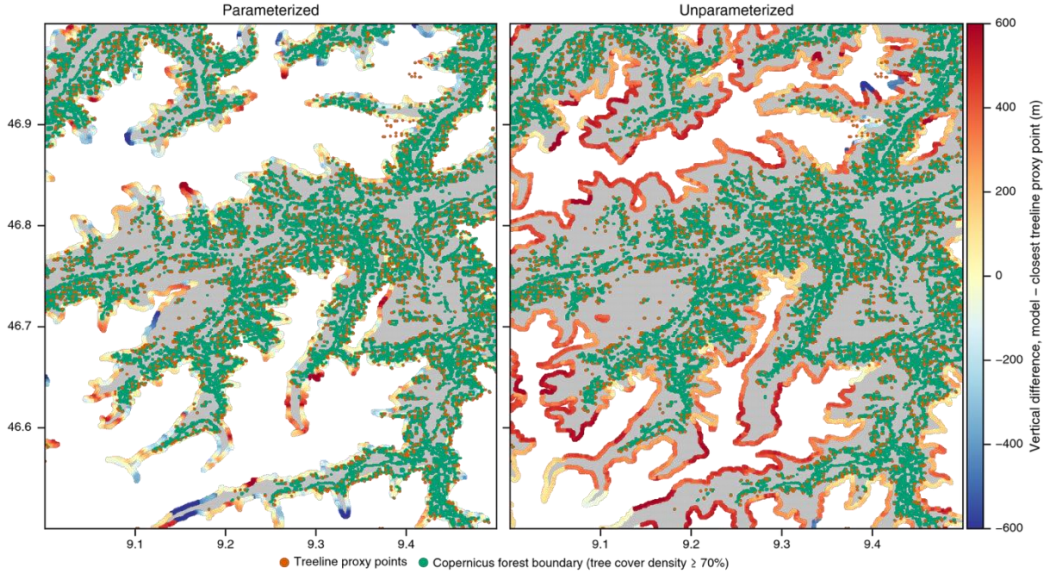

Figure 4. Vertical distance between predicted and nearest observed treeline points between parameterized model and unparameterized model predictions based on 1981–2010 climate normals at 90 m resolution for longitude 9.0–9.5, and latitude 46.5–47.0. In green: Copernicus tree cover points selected with a 70 % tree cover mask. In orange: representatives of the natural treeline from the Copernicus tree cover mask, representing the highest recorded tree presence within a 20 x 20 pixel moving window with a stride of 8 and expected to better approximate the natural

https://doi.org/10.5194/egusphere-2026-4919
Preprint. Discussion started: 17 September 2026

460 treeline position despite land use. In gray: predicted tree-covered area with the corresponding BIOME4 model instance representing the potential natural forest area.

3.2 Case study 2. Modeling a new succulent biome

Succulence is a morphological adaptation that enables plants to cope with chronic water scarcity (Gibson, 2012; Grace, 2019; Willert, 1992). The origin and diversification of succulents is thought to be associated with a global expansion
465 of aridity during the late Miocene/Pliocene, about 10–5 Ma (Arakaki et al., 2011; Hernández-Hernández et al., 2014). We define the succulent biome as frost-free, fire-intolerant, and characterized by strongly seasonal rainfall deficit with long-lasting drought periods, and with vegetation characterized by a high cover proportion of tall (> 1 m) stem succulents, often deciduous, displaying reduced leaf area (Ávila-Lovera & Ezcurra, 2016; Gagnon et al., 2019). The succulent biome is expected to dominate across the dry tropics (Ávila-Lovera & Ezcurra, 2016). Despite their
470 adaptation to chronic water limitation and their role in shaping dry-tropical ecosystems, succulent lineages remain underrepresented in mechanistic vegetation models, constraining assessments of biome-climate interactions in arid environments (Grace, 2019; Midgley & Bond, 2015).

We integrate functional traits into the definitions of a stem succulent PFT and a succulent biome in Biome.jl, and we model them together with the BIOME4 PFTs using the new competition logic. We parameterized the stem succulent
475 PFT with a long leaf longevity to mimic the photosynthetic stem, extremely shallow rooting depth, tight stomatal control, and CAM-like respiration, reflecting slow tissue turnover, rapid uptake after intermittent rainfall, and high water-use efficiency (Ávila-Lovera & Ezcurra, 2016; Bobich & North, 2009). Climate tolerance limits were set to enforce strong frost intolerance and preference for semi-arid conditions, restricting establishment to warm, dry environments and excluding both hyper-arid and cold-desert regions. All parameters for the succulent PFT are given
480 in Table A1. These limits were confirmed by a grid search parameter estimation using the GBIF-based stem succulent occurrence map modelled by Ringelberg et al. (2020a) and based on more than 1,000 species primarily from the family Burseraceae and the genera *Bourreria*, *Caesalpinia*, *Gambelia*, *Leucaena*, *Parkinsonia*, *Pictetia*, *Prosopis*, *Sideroxylon*, and *Thamnosma* (GBIF, 2026) (Fig. A3). Most of the parameterization was done manually, building upon traits and constraints from the desert woody PFT of the BIOME4 model and basing the logic on established
485 knowledge of succulent traits (Haxeltine & Prentice, 1996; Kaplan, 2001). We also introduced a "succulent biome" and implemented a custom biome-assignment rule that attributes this biome when competition does not suppress stem succulent dominance.

We then calculated recall, precision, and true skill score (TSS) of our model against a raster of the modelled stem-succulent (< 1 m) biome distribution map from Ringelberg et al. (2020a) in predicting the range of stem succulents.
490 We selected only cells where all ensemble members agreed on presence, a stricter criterion than the original study, which classified a cell as suitable when at least one-third of models predicted the stem-succulent biome (Ringelberg et al., 2020b). We calculated these metrics only over regions where succulents have evolved, removing Australia and Asia from the score computation.

https://doi.org/10.5194/egusphere-2026-4919
Preprint. Discussion started: 17 September 2026

3.2.1 Results

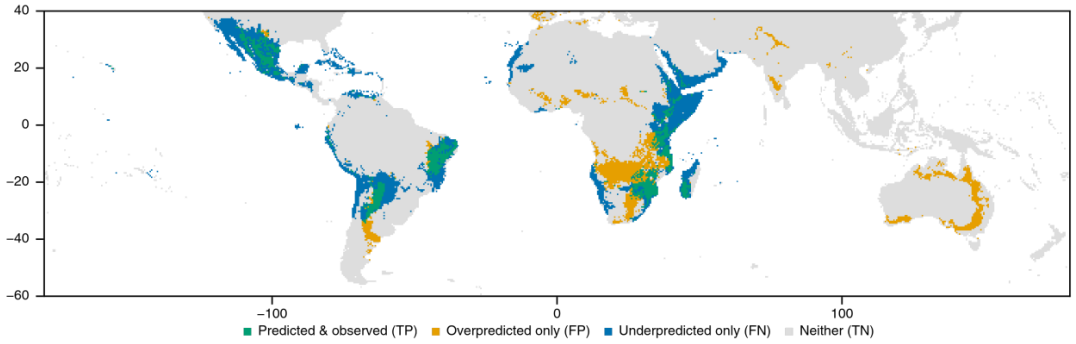

Figure 5. Predicted stem succulence presence overlaid with modelled distribution of the main stem-succulent genera and families as collected by Ringelberg and colleagues (2020a). Colors highlight: in green, the agreement between the two maps (TP, true positives); in orange and blue, overprediction of the extent of the stem-succulent biome modelled with Biome.jl (FP, false positives) and underprediction (FN, false negatives), respectively. Gray represents true negatives (TN), where the PFT is never predicted.

Biome.jl simulations effectively depict the highly fragmented, pantropical distribution of the succulent biome across the Neotropics, Africa, Arabia, and Madagascar, with a near absence from most of Asia except for Pakistan and north-western India (Hernández-Hernández et al., 2014; Lavin et al., 2004; Ringelberg et al., 2020b). Model agreement was strongest in core succulent regions such as the Caatinga and Chaco in South America, southern African drylands, the Sonoran Desert, and Madagascar, where predicted presence closely overlaps with dense occurrence clusters. The model also predicted succulent occurrence in Australia. There, stem succulents are naturally absent, yet the spread of invasive stem succulents from various genera has been recorded (Novoa et al., 2015).

Within a 1-pixel tolerance radius, to account for pixel heterogeneity and edge effects, our model achieved 0.54 recall, 0.32 precision, and 0.48 TSS when compared to the Ringelberg ensemble map. The model was efficient at predicting correct distribution but remained too conservative, omitting parts of the succulent range in hyper-dry areas and subtropical regions. Prediction errors were concentrated along ecotones and in regions with mixed fire regimes, mostly mixing up savanna and succulent biomes. Because the succulent biome is known to be fire-intolerant, incorporating a fire regime map as a model input could better constrain its predicted extent and reduce these errors. We consider this a successful proof-of-concept that illustrates how a new PFT and biome can be added in Biome.jl, and it could be significantly improved with targeted parameterization efforts based on observed, rather than modelled, distribution maps.

4 Discussion

Capturing the processes that drive biome distributions requires considering climatic constraints, ecophysiological process simulations and tolerances definitions, and competitive interactions across different spatial and temporal scales (Mucina, 2019). We introduced Biome.jl, a Julia-based modeling framework for developing, comparing, and

https://doi.org/10.5194/egusphere-2026-4919
Preprint. Discussion started: 17 September 2026

testing alternative biome definitions, and have shown that it can do so efficiently. Biome.jl is built around a fully customizable mechanistic framework that separates the physiological core from user-defined PFT definitions, competition logic, and biome attribution rules, with a reimplementation of BIOME4 provided as a reference configuration, alongside climate-envelope biome classifications. Validation against the RESOLVE ecoregions and GLCNMO reference datasets confirms that this flexibility does not compromise predictive performance: the new competition logic performs similarly to, and in some cases slightly better than, the original BIOME4 scheme (Table 2). The case studies demonstrate that the modeling framework can be parameterized to account for continental differences in PFT distributions and extended to incorporate new PFTs and biome concepts, such as the stem-succulent PFT and biome, with minimal structural changes. With this added flexibility, Biome.jl offers a modular platform, created to explore competing biome ideas, run predictions under different climate scenarios, and integrate biome simulations with palaeoecological and evolutionary research.

Comparing multiple biome distributions helps identify which processes are key to shaping global vegetation patterns (Grimm & Railsback, 2012). Biome.jl enables this comparison by running the same climatic inputs through multiple schemes, so differences in predicted biomes can be directly linked to model assumptions. We suggest extending the framework by incorporating the global biome catalog synthesized by Fischer et al. (2022) alongside more classical biome schemes (e.g., Olson et al., 2001; Whittaker, 1970). This extension would enable even more biome definitions to be represented within a single, internally consistent modeling environment rather than as independent static maps. Because the framework is open-source and PFT definitions are modular, community-contributed PFT and biome configurations could be shared and versioned collaboratively, expanding the catalog of testable biome concepts and fostering community-driven model development.

Thanks to Julia's high computational efficiency, Biome.jl enables ensemble simulations of biome responses to climate change, similar to ensemble approaches used in climate and species distribution models. Variation in the spatial representation of biomes or PFTs as input to Earth system models can strongly influence climate simulation results, especially in arid regions (Poulter et al., 2011). It can therefore be meaningful to run different PFT or biome schemes as input into simulations of climate models through time. Running Biome.jl with different climate model data and creating ensemble simulations would allow mapping and explicitly quantifying uncertainties in projected biome shifts. At the same time, as an equilibrium framework, Biome.jl shares limitations common to the BIOME suite (Prentice et al., 1992; Kaplan et al., 2003): it does not explicitly resolve transient vegetation dynamics, short-term responses to disturbance, or physiological acclimation (Haywood et al., 2002). It does not represent the saturation of plant photosynthesis to rising atmospheric CO_2 nor include nitrogen and phosphorus cycles. Applications of Biome.jl to future-climate scenarios therefore show strong signs of CO_2 fertilization unconstrained by the model, representing increasing uncertainty in projected biome shifts. These limitations contrast with those of dynamic global vegetation models like the LPJ-GUESS suite (Smith et al., 2014), which resolve short time steps, carbon and nitrogen cycling, and disturbance regimes, but at significant computational expense. Biome.jl fills a complementary niche: because it does not require as much computational overhead, it supports more detailed PFT and biome definitions and can be adjusted more flexibly. Its simplicity and speed make it a practical platform for exploratory hypothesis testing and

https://doi.org/10.5194/egusphere-2026-4919
Preprint. Discussion started: 17 September 2026

scenario planning, while short-term projections may still require coupling with or comparison to dynamic models. Future development could address some of these gaps by adding CO_2 response functions calibrated against FACE experiment data (Norby & Zak, 2011) or by incorporating precipitation seasonality, nutrient limitation, and disturbance regimes (fire, grazing) as additional processes and constraints to the Biome.jl framework (Beigaitė et al., 2022; Hernández-Hernández et al., 2014). In addition, biome identity is evaluated independently of historical and dispersal processes in Biome.jl. This is illustrated by the succulent case study, in which we use Biome.jl to identify regions where climate and soil conditions support stem-succulent dominance, but where native succulent lineages are absent. Previous work has shown that the climates of invaded regions closely match those of cacti's native ranges (Novoa et al., 2015), supporting the interpretation that this mismatch reflects the availability of lineages rather than climatic limitations. Converting potential biomes into historically informed biome distributions, therefore, requires additional information on lineage presence, dispersal pathways, and connectivity, as commonly applied in range-shift and connectivity modeling (Koen et al., 2014; Alagador et al., 2016). If considered accordingly, the biome distributions generated by Biome.jl can be integrated with evolutionary models (e.g., Hagen et al., 2021; Keppel et al., 2012; L. Ma et al., 2022), connectivity analyses (e.g., (Ding et al., 2025; Koen et al., 2014), or approaches to consider migration pathways (e.g., Alagador et al., 2016; Nobis & Normand, 2014) to distinguish where a biome could occur climatically from where specific PFTs and their representative lineages were able to disperse to and where biomes themselves could act as corridors for other species. Palaeoecological applications of Biome.jl rely on the assumption that PFT tolerances are conserved, and that past vegetation responded to climate similarly to modern vegetation (Haywood et al., 2002). Rather than treating this solely as a limitation, paleorecords could be used to inform PFT definitions representing vegetation types that no longer exist, extending the framework beyond modern analogs. The parameter estimation framework developed here provides a tool for this: calibrating PFT tolerances against paleorecords across time slices could allow tracking how individual functional types spread and adapted to different niches over geological time, providing a link between biome modeling and macroevolutionary analyses. Taken together, these extensions position Biome.jl as a tool suitable for testing biome theories, conducting comparative analyses of different biome and PFT classifications, and answering broader questions about convergence, diversification, and the distribution of global vegetation.

Using illustrative case studies, we have demonstrated the flexibility of Biome.jl, validated its predictions, and showcased the use of the engine to extend biome concepts. The case studies are not intended to represent thorough ecological analyses, but rather to demonstrate how mechanistic assumptions can be modified and evaluated against independent data using Biome.jl. Case study 1 demonstrates the value of parameterizing Biome.jl for comparing species pools, with implications for biogeography and evolutionary studies (Moncrieff et al., 2016). While the parameterization focused on plant functional types that are primarily limited by climate, extending this approach to PFTs influenced by both environmental filtering and competition will require careful treatment to avoid overfitting. Case study 2 shows how Biome.jl can be extended to represent new biome concepts with minimal structural overhead. New PFTs can be defined using empirical information and combined to derive biomes tailored to specific research questions. In this study, the stem succulent biome (Ringelberg et al. 2020b) was introduced as a deliberately simplified example to demonstrate how a new PFT and associated biome can be added to the framework without much effort. In

https://doi.org/10.5194/egusphere-2026-4919
Preprint. Discussion started: 17 September 2026

this context, Biome.jl identifies regions of climatic suitability relevant to interpreting biome evolution and assessing environments susceptible to invasion. By keeping biome extensions modular, Biome.jl shifts the main effort from model modification to ecological interpretation and hypothesis testing.

5 Conclusions

Biome.jl introduces a new philosophy to biome modeling. We demonstrated the ease and success of generating and applying quantitative new parameterization in Biome.jl for a case study on optimizing the simulation of treeline location in the Swiss Alps, and in modeling the global distribution of a new desert succulent plant functional type and biome. As a modular platform for comparing alternative biome classifications and identifying patterns that persist across models, datasets, and assumptions, Biome.jl thus represents a testbed for hypothesis testing and constitutes an important step towards the development of a unified biome concept.

https://doi.org/10.5194/egusphere-2026-4919
Preprint. Discussion started: 17 September 2026

Appendix A

(a) Koeppen-Geiger

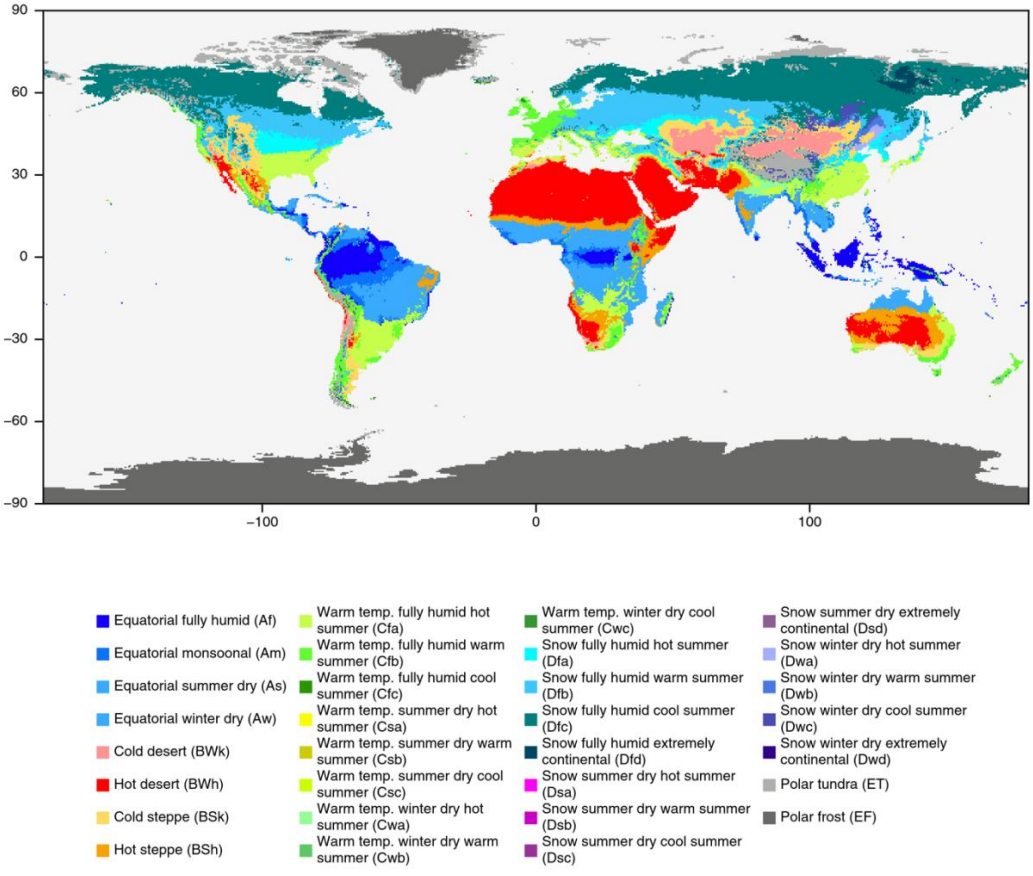

https://doi.org/10.5194/egusphere-2026-4919
Preprint. Discussion started: 17 September 2026

(b) Thornthwaite

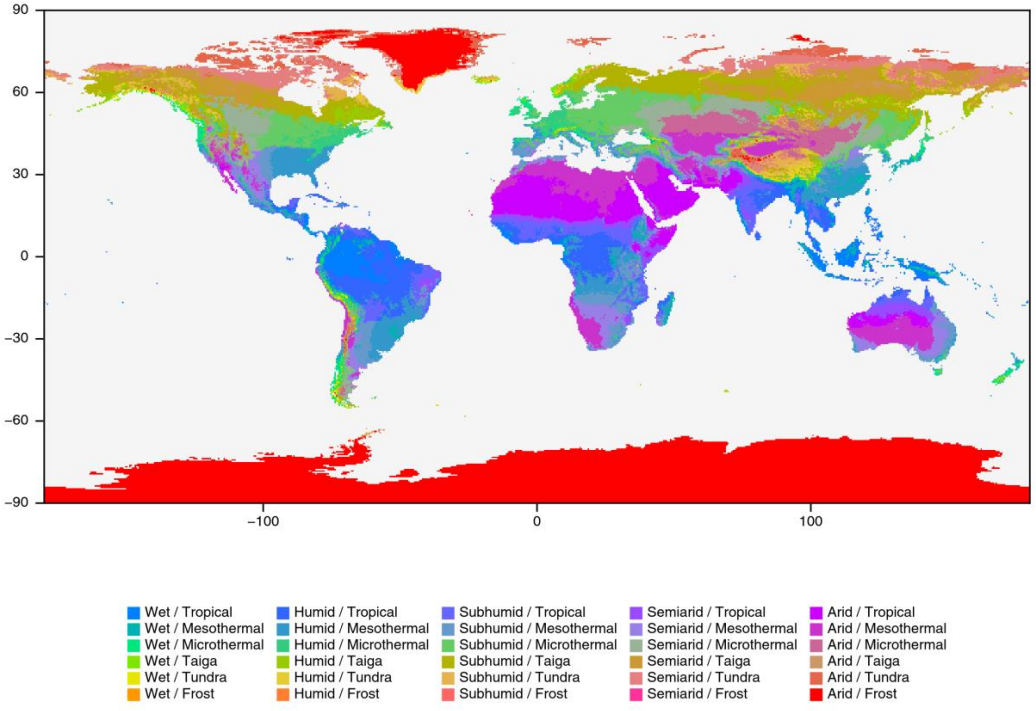

https://doi.org/10.5194/egusphere-2026-4919
Preprint. Discussion started: 17 September 2026

(c) Troll-Paffen

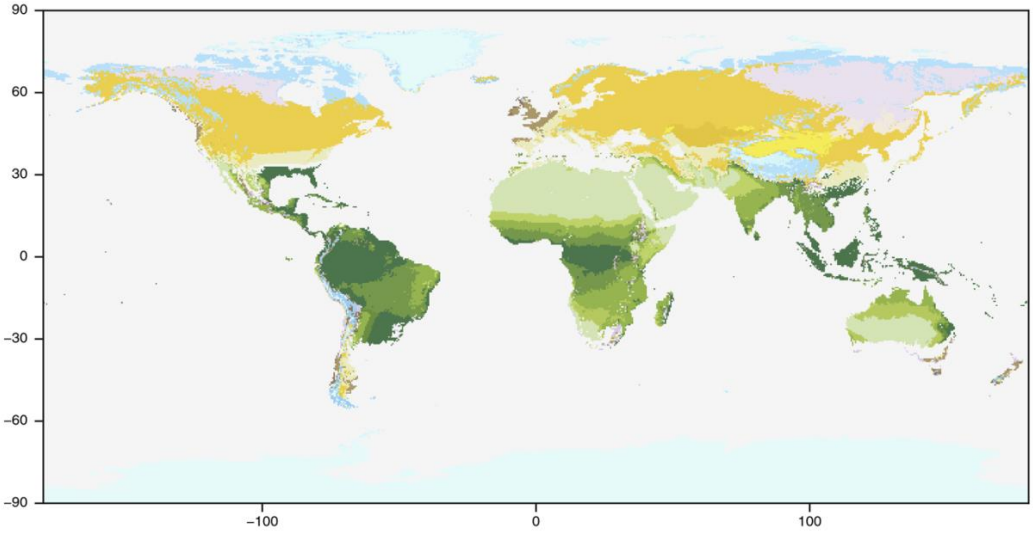

- Polar ice-deserts
- Polar frost-debris belt
- Tundra
- Sub-polar tussock grassland/moors
- Oceanic humid coniferous woods
- Continental coniferous woods
- Highly continental dry coniferous woods
- Evergreen broad-leaved/mixed woods
- Oceanic deciduous broad-leaved/mixed woods
- Sub-oceanic deciduous broad-leaved/mixed woods
- Sub-continental deciduous broad-leaved/mixed woods
- Continental decid. broad-leaved/mixed woods + wooded steppe
- Highly continental decid. broad-leaved/mixed woods + wooded steppe
- Decid. broad-leaved/mixed wood + wooded steppe
- Thermophile dry wood + wooded steppe
- Humid deciduous broad-leaved/mixed wood
- High grass-steppe with perennial herbs
- Humid steppe with mild winters
- Short grass/dwarf shrub/thorn-steppe
- Steppe: short grass, dwarf shrubs, thorns
- Central/East-Asian grass + dwarf shrub steppe
- Semi-desert/desert with cold winters
- Semi-desert/desert with mild winters
- Sub-tropical hard-leaved/coniferous wood
- Sub-tropical grass + shrub-steppe
- Sub-tropical thorn/succulents-steppe
- Sub-tropical steppe with short grass
- Sub-tropical semi-deserts/deserts
- Sub-tropical high-grassland
- Sub-tropical humid forests
- Evergreen tropical rain forest
- Rain-green humid forest
- Half-deciduous transition wood
- Rain-green dry wood + savannah
- Tropical thorn-succulent wood + savannah
- Tropical dry climates, humid winter months
- Tropical semi-deserts/deserts

https://doi.org/10.5194/egusphere-2026-4919
Preprint. Discussion started: 17 September 2026

(d) Wissmann

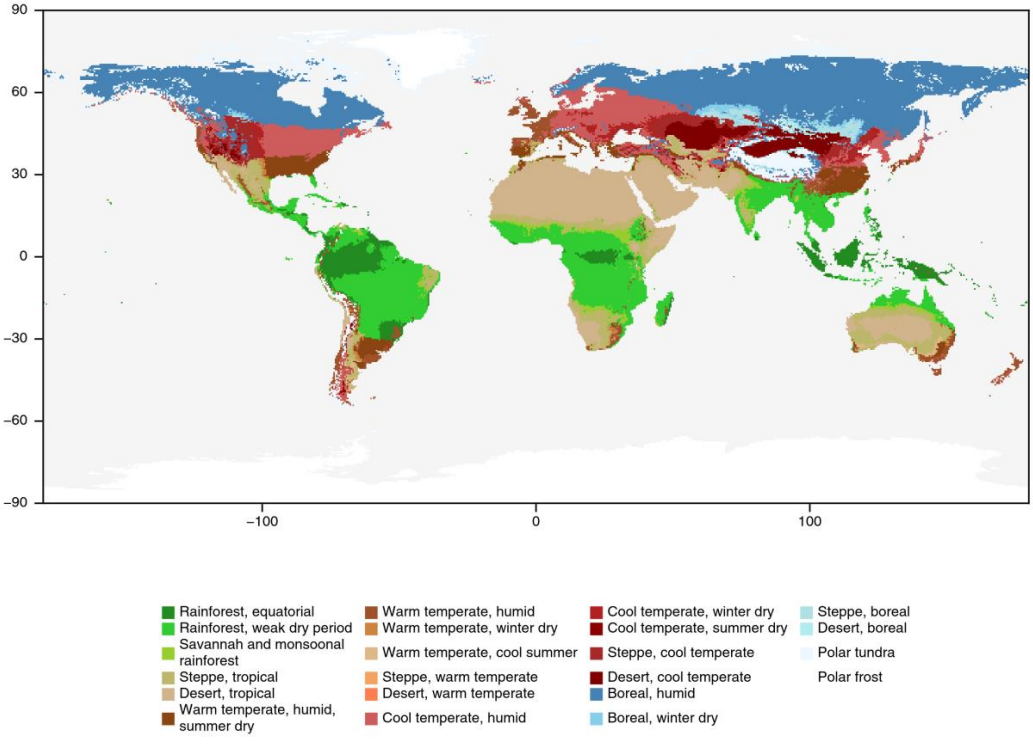

610

https://doi.org/10.5194/egusphere-2026-4919
Preprint. Discussion started: 17 September 2026

(e) BIOME4 (reference)

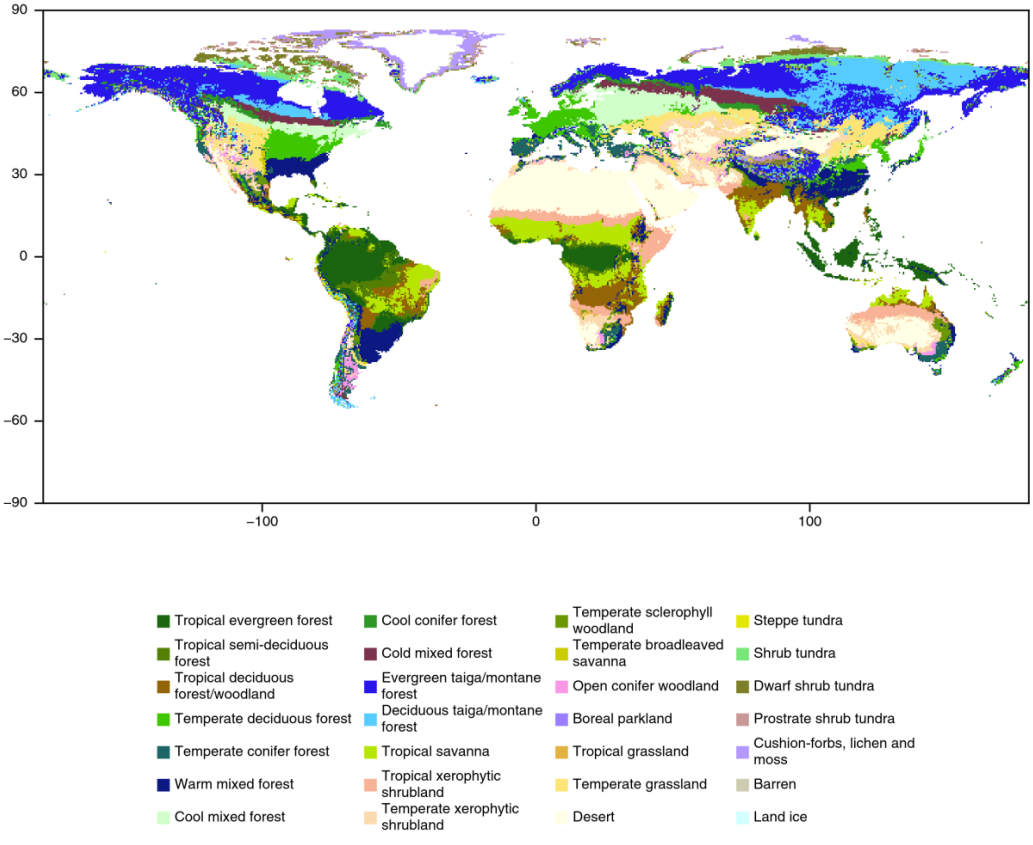

https://doi.org/10.5194/egusphere-2026-4919
Preprint. Discussion started: 17 September 2026

(f) BIOME4 with modified competition

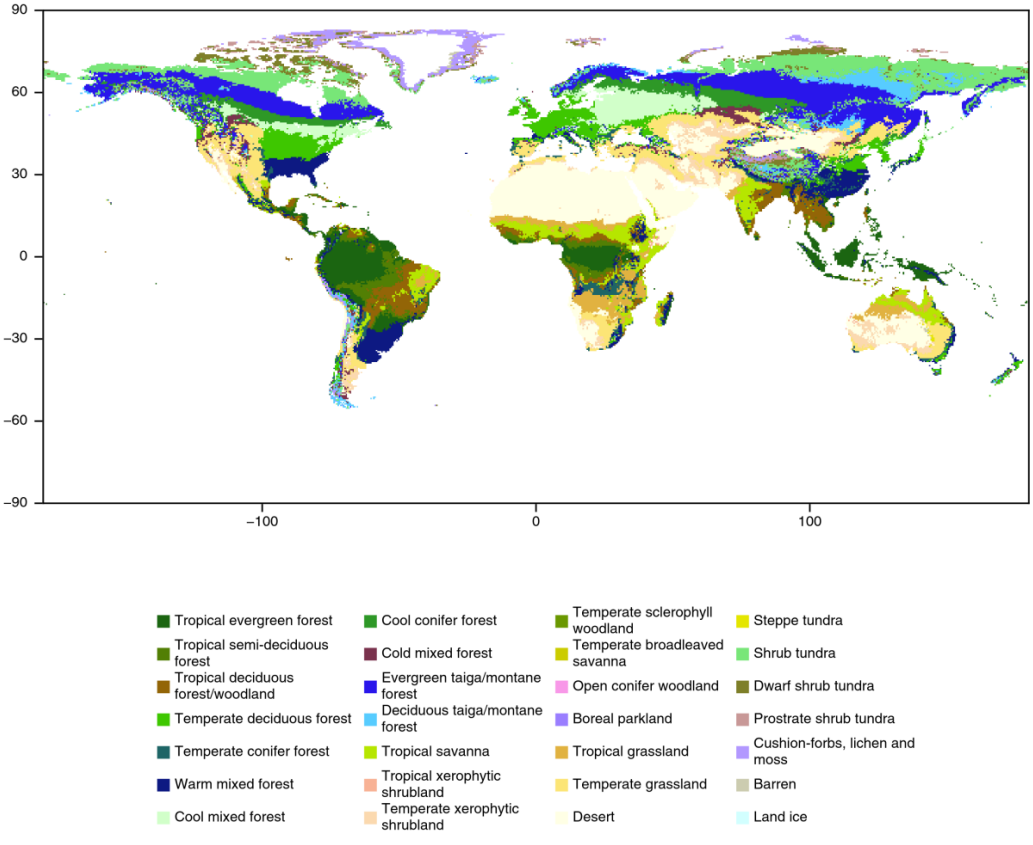

615

https://doi.org/10.5194/egusphere-2026-4919
Preprint. Discussion started: 17 September 2026

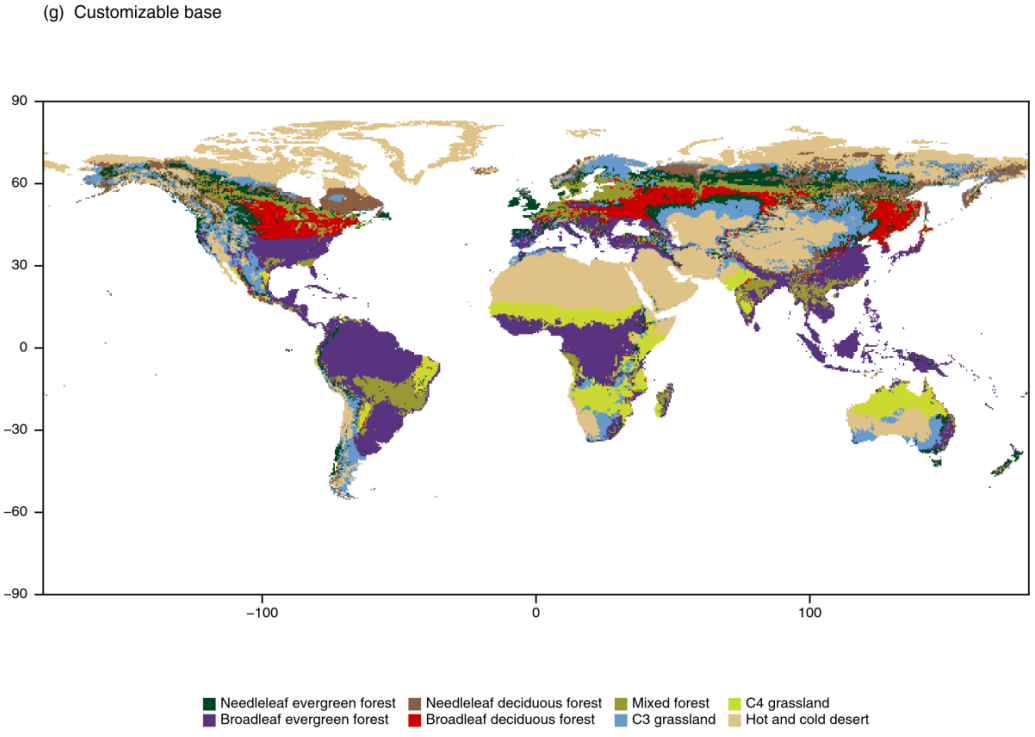

Figure A1. Possible model outputs from the Biome.jl engine. From top to bottom: (a) Köppen-Geiger scheme, (b) Thornthwaite scheme, (c) Troll-Paffen scheme, (d) Wissmann scheme, (e) BIOME4, (f) BIOME4 with generalized competition, (g) Customizable base.

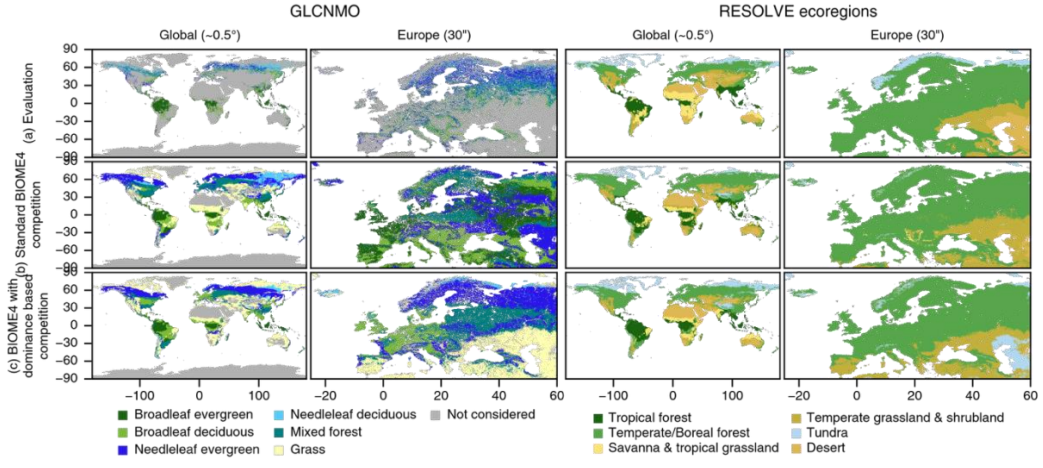

620

Figure A2. Comparison of observed and modeled biome distributions at two spatial resolutions. (a) Vegetation distribution maps aggregated from the GLCNMO and RESOLVE ecoregions datasets. (b) Vegetation distribution simulated with the original BIOME4 competition scheme. (c) Vegetation distribution simulated with BIOME4 using

https://doi.org/10.5194/egusphere-2026-4919
Preprint. Discussion started: 17 September 2026

the modified dominance-based competition subroutine implemented in Biome.jl. Results are shown globally at 0.5° resolution (left panels) and for Europe at 30” resolution (right panels). Colors indicate major vegetation classes into which GLCNMO, RESOLVE ecoregions, and BIOME4 were aggregated for comparison. For GLCNMO: broadleaf evergreen, broadleaf deciduous, needleleaf evergreen, needleleaf deciduous, mixed forest, and grass, and for RESOLVE: tropical forest, temperate and boreal forest, savanna and tropical grassland, temperate grassland and shrubland, tundra, and desert.

Table A1. Functional traits and parameter values defining the Succulent PFT

https://doi.org/10.5194/egusphere-2026-4919
Preprint. Discussion started: 17 September 2026

Parameter	Name in model	Value for succulents	Description / Biological motivation for value in succulent case study
Phenological type	phenological_type	2	deciduous phenology, consistent with many stem succulents
Maximum canopy conductance	max_min_canopy_conductance	0.05	very tight stomatal regulation; high water-use efficiency (CAM-like)
Maximum daily transpiration	Emax	8	kept from woody desert defaults in BIOME4
Fraction of roots in top soil	root_fraction_top_soil	0.9	extremely shallow, opportunistic roots enabling rapid uptake after rain
Leaf Longevity	leaf_longevity	30	long-lived tissues; slow turnover typical of succulents
Sapwood_respiration	sapwood_respiration	2	no true sapwood
Optimal Ci/Ca ratio for photosynthesis	optratioa	0.7	kept from woody desert defaults in BIOME4
Stomatal Sensitivity	kk	0.3	stomatal sensitivity parameter
C4 Photosynthesis	c4	FALSE	succulents use CAM or C_3 metabolism
Fire resistance threshold	threshold	0.25	low fire tolerance; maintains suppression in fire-prone savannas
Reference temperature for growth initiation	t0	10	
Temperature response curve	tcurve	1	
Sapwood maintenance respiration	respfact	1.6	elevated respiration reflecting CAM energetics
Allocation factor for leaf vs litter mass	allocfact	1	
Grass	grass	FALSE	stem-succulent growth form, not grass-like
Dominance Factor	dominance_factor	2	
Minimum LAI	minimum_lai	2	sparse canopy typical of tall succulents
Climate constraints			
Temperature of the coldest month	tcm	[5, +∞]	requires mild winter cold-month temperatures
Absolute minimum temperature	tmin	[-5, +∞]	strong intolerance to freezing
GDD_5	gdd5	[–∞, +∞]	no constraint
GDD_0	gdd0	[–∞, 10000]	
Temperature of the warmest month	twm	[–∞, +∞]	no warm-month constraint
Maximum snow depth	maxdepth	[–∞, +∞]	no snow depth constraint (not relevant)
Site water balance	swb	[5, 44]	semi-arid environments, excludes hyper-arid deserts (< 5 % of field capacity)

https://doi.org/10.5194/egusphere-2026-4919
Preprint. Discussion started: 17 September 2026

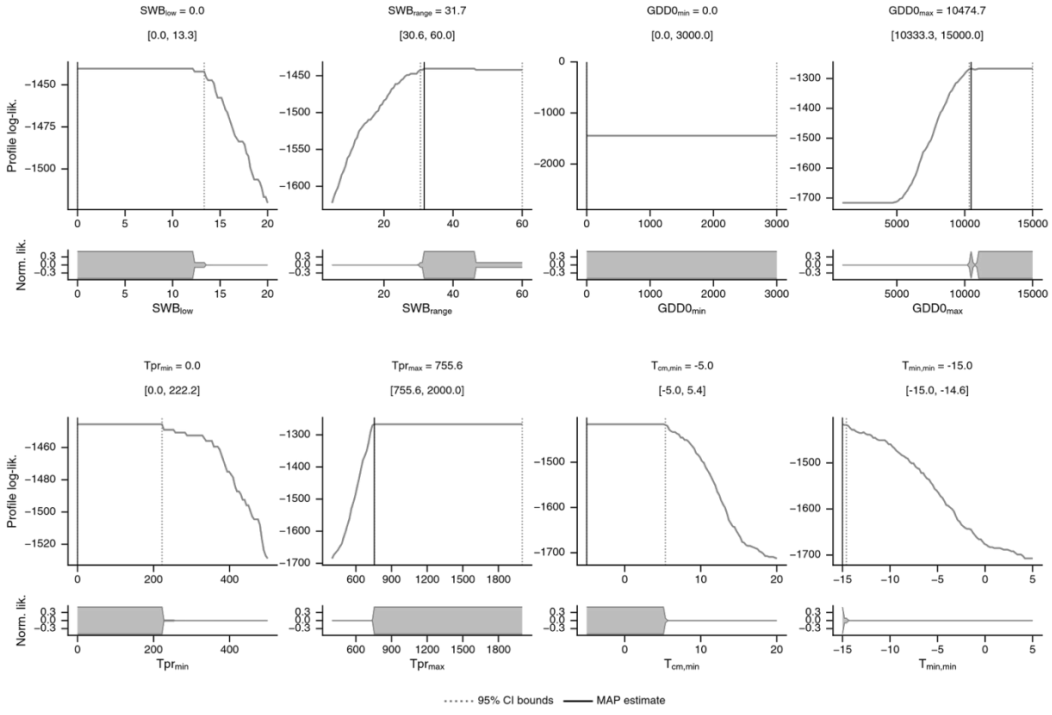

Figure A3. Results of parameter estimation using a grid search approach for climatic constraint parameters as profile log likelihood (Profile log. lik.) and normalized likelihood (Norm. lik.) for the lower bound of the Temperature of the coldest month ($T_{CM,\ min}$), absolute minimum temperature ($T_{min,\ min}$), the upper and lower bounds of the site water balance as percentage of the field capacity (swb_{low} and swb_{high}), the upper and lower bounds of the total yearly precipitation (tpr_{min} and tpr_{max}, and bounds of growing degree days above 0°C ($GDD_{0,\ min}$ and $GDD_{0,max}$) the stem-succulent PFT based on modelled distribution data from Ringelberg and colleagues (2020a). Vertical bars indicate the selected parameter value, where MAP stands for maximum a posteriori estimate, the parameter value that maximizes the posterior distribution, and its 95 % confidence interval. Acc stands for accuracy, the fraction of sampled pixels whose predicted presence/absence matched the ground truth at the MAP parameter value.

Appendix B. Calculations of the competitive dominance score

For each PFT, noted p in the following equations, the fundamental niche N_p is defined as a set of admissible intervals with a lower bound $l_{p,j}$ and an upper bound $u_{p,j}$ for each predictor j.

$$N_p = \{[l_{p,j}, u_{p,j}]\} \mid j \in \{t_{cm}, t_{min}, GDD_5, GDD_0, t_{wm}, maxdepth\} \quad \text{(B1)}$$

These bounds may be open, i.e. $l_{p,j} = -\infty$, and/or $u_{p,j} = +\infty$ or set to a specific value.

The potential fitness of each PFT in the grid cell is normalized by its distance from its optimal conditions. Indeed, each grid cell x is represented by a vector of the same environmental predictors (Table 1)

$$x = (t_{cm}, t_{min}, GDD_5, GDD_0, t_{wm}, maxdepth) \quad \text{(B2)}$$

https://doi.org/10.5194/egusphere-2026-4919
Preprint. Discussion started: 17 September 2026

The distance of a pixel value x_j to the admissible interval of a predictor j is defined as:

$$d_{p,j}(x_j) = l_{p,j} - x_j \; if \; x_j < l_{p,j}$$

$$d_{p,j}(x_j) = 0 \; if \; l_{p,j} < x_j < u_{p,j} \quad \text{(B3)}$$

$$d_{p,j}(x_j) = x_j - u_{p,j} \; if \; x_j > u_{p,j}$$

Each distance is normalized by a predictor-specific tolerance parameter $s_{p,j,}$ which depends on the natural range of the parameter. For example, absolute minimum temperature would naturally range between -60 and 20 °C, while maximum snow depth would range between 0 and 20m, and this would affect the value of the tolerance parameter. When both lower and upper bounds of the predictor are defined, tolerance is set proportional to the width of the admissible interval, such that wider niches correspond to broader tolerance. This value is constrained within predictor-specific minimum and maximum limits to avoid unrealistically sharp responses. When one or both bounds are unbounded, tolerance range is assigned a fixed default value ($t_{cm:}$ 4.0 °C, t_{min}: 4.0 °C, GDD_5: 800 °C day^{-1}, GDD_0: 800 °C day^{-1}, t_{wm}: 2.5 °C, maxdepth: 7.5 cm) reflecting the typical scale of variation of the predictor.

The squared standardized distance of a pixel $\mathbf{x}$ to the fundamental niche of the PFT is

$$D_p^2(x) = \sum_j \left(\frac{d_{p,j}(x_j)}{s_{p,j}}\right)^2 \quad \text{(B4)}$$

The fitness level of the PFT in this environmental cell is then computed using a Gaussian-shaped kernel.

$$S_p(x) = e^{\left(-\frac{1}{2}D_p^2(x)\right)} \quad \text{(B5)}$$

The competitive ability of the PFT in each pixel C(x) is then computed by multiplying this fitness level by the calculated maximum sustainable NPP and its dominance class value D

$$C(x) = S_p(x) \cdot NPP \cdot \frac{1}{D} \quad \text{(B6)}$$

Code availability

The current version of Biome.jl is openly available at https://github.com/clechartre/Biome.jl under the GPLv3 license. The R interface biomeR is available at https://github.com/clechartre/biomeR, also under the GPLv3 license. The original BIOME4 Fortran source code is available at https://zenodo.org/records/11270258 (Kaplan, 2024).

The exact version v0.1.0 of the model used to produce the results used in this paper is archived on Zenodo at https://doi.org/10.5281/zenodo.21921098 (Lechartre et al., 2026a), and biomeR is archived at https://doi.org/10.5281/zenodo.22658759 (Lechartre et al., 2026b).

Simulation scripts for the case studies presented in this paper are available at https://github.com/clechartre/Biome.jl/examples/case_studies and within the Zenodo archive of the Biome.jl model.

https://doi.org/10.5194/egusphere-2026-4919
Preprint. Discussion started: 17 September 2026

Data availability

The global biome maps from Ma et al. (2023) used for model evaluation are available at https://zenodo.org/records/15102025. The Swiss case study uses 90 m resolution climate data that are publicly available on the CHELSA website under https://www.chelsa-climate.org/datasets/chelsach-highres-climatologies and https://www.doi.org/10.16904/envidat.689. Swiss National Forest Inventory leaf type mixture proportion data are archived under the DOI https://doi.org/10.16904/1000001.6 (Waser et al., 2025). CHELSA V2 climatologies (1980–2010) used as climate inputs for the succulent case study are available at https://www.chelsa-climate.org/datasets/chelsa_climatologies and https://www.doi.org/10.16904/envidat.228. Stem succulent distribution maps used as ground truth are provided in the supplementary data of Ringelberg et al. (2020b) at https://doi.org/10.5061/dryad.08kprr4zs (Ringelberg et al., 2020a).

Author contributions

CMSL, VB, PB, and NEZ conceived the study and designed the methodology.
NEZ acquired and provided the funding necessary for the realization of this study.
JOK designed the original BIOME4 software and advised, together with VB, PB, and NEZ, on new developments.
CMSL implemented the modeling framework and developed the parameterization methodology with technical advice from VB.
CMSL conducted simulations, performed the formal analysis, and interpreted the results.
DNK provided the climatic data necessary for Case study 1.
CMSL wrote the original draft, and all authors critically revised the manuscript.

Competing Interest

The authors declare no conflict of interest.

Acknowledgments

This work is part of the project “Predicting hotspots of climate change impacts on ecosystems from an eco-evolutionary biome framework,” supported by the Swiss National Foundation (TMAG_3 #216072). The computations of this study were performed on the Hyperion computing cluster, which is supported by the Swiss Federal Institute for Forest, Snow, and Landscape WSL.
We would like to acknowledge the use of Anthropic’s Claude in editing the code used to generate the figures and polishing the manuscript concerning wording and grammar. The authors reviewed and edited all AI-generated content manually.

https://doi.org/10.5194/egusphere-2026-4919
Preprint. Discussion started: 17 September 2026

Financial support

This work was supported by the Swiss National Science Foundation (SNSF) with the Advanced Grant (TMAG_3 #216072).

References

Ahti, T., Hämet-Ahti, L., and Jalas, J.: Vegetation zones and their sections in northwestern Europe, Ann. Bot. Fenn., 5, 169–211, 1968.

Alagador, D., Cerdeira, J. O., and Araújo, M. B.: Climate change, species range shifts and dispersal corridors: an evaluation of spatial conservation models, Methods Ecol. Evol., 7, 853–866, https://doi.org/10.1111/2041-210X.12524, 2016.

Anderegg, L. D. L., Griffith, D. M., Cavender-Bares, J., Riley, W. J., Berry, J. A., Dawson, T. E., and Still, C. J.: Representing plant diversity in land models: an evolutionary approach to make "Functional Types" more functional, Glob. Change Biol., 28, 2541–2554, https://doi.org/10.1111/gcb.16040, 2022.

Arakaki, M., Christin, P.-A., Nyffeler, R., Lendel, A., Eggli, U., Ogburn, R. M., Spriggs, E., Moore, M. J., and Edwards, E. J.: Contemporaneous and recent radiations of the world's major succulent plant lineages, P. Natl. Acad. Sci. USA, 108, 8379–8384, https://doi.org/10.1073/pnas.1100628108, 2011.

Ávila-Lovera, E. and Ezcurra, E.: Stem-succulent trees from the Old and New World tropics, in: Tropical Tree Physiology, Springer, https://doi.org/10.1007/978-3-319-27422-5_3, 2016.

Aziz, G., Minallah, N., Saeed, A., Frnda, J., and Khan, W.: Remote sensing based forest cover classification using machine learning, Sci. Rep., 14, 69, https://doi.org/10.1038/s41598-023-50863-1, 2024.

Bachelet, D., Lenihan, J., Daly, C., Neilson, R., Ojima, D., and Parton, W.: MC1: a dynamic vegetation model for estimating the distribution of vegetation and associated ecosystem fluxes of carbon, nutrients, and water, General Technical Report PNW-GTR-508, US Department of Agriculture, Forest Service, Pacific Northwest Research Station, Portland, OR, USA, 2001.

Bai, M., Peng, P., Zhang, S., Wang, Xueman, Wang, Xiao, Wang, J., and Pellikka, P.: Mountain forest type classification based on one-dimensional convolutional neural network, Forests, 14, 1823, https://doi.org/10.3390/f14091823, 2023.

Beck, H. E., McVicar, T. R., Vergopolan, N., Berg, A., Lutsko, N. J., Dufour, A., Zeng, Z., Jiang, X., van Dijk, A. I. J. M., and Miralles, D. G.: High-resolution (1 km) Köppen-Geiger maps for 1901–2099 based on constrained CMIP6 projections, Sci. Data, 10, 724, https://doi.org/10.1038/s41597-023-02549-6, 2023.

Beierkuhnlein, C. and Fischer, J.-C.: Global biomes and ecozones – conceptual and spatial communalities and discrepancies, Erdkunde, 75, 249–270, 2021.

Beigaitė, R., Tang, H., Bryn, A., Skarpaas, O., Stordal, F., Bjerke, J. W., and Žliobaitė, I.: Identifying climate thresholds for dominant natural vegetation types at the global scale using machine learning: average climate versus extremes, Glob. Change Biol., 28, 3557, https://doi.org/10.1111/gcb.16110, 2022.

Bezanson, J., Karpinski, S., Shah, V. B., and Edelman, A.: Julia: a fast dynamic language for technical computing, arXiv [code], arXiv:1209.5145, 2012.

Bobich, E. and North, G.: Structural implications of succulence: architecture, anatomy, and mechanics of photosynthetic stem succulents, pachycauls, and leaf succulents, in: Perspectives in Biophysical Plant Ecophysiology, 3–38, 2009.

Box, E. O.: Factors determining distributions of tree species and plant functional types, Vegetatio, 121, 101–116, https://doi.org/10.1007/BF00044676, 1995.

Brun, P., Zimmermann, N. E., Hari, C., Pellissier, L., and Karger, D. N.: Global climate-related predictors at kilometer resolution for the past and future, Earth Syst. Sci. Data, 14, 5573–5603, https://doi.org/10.5194/essd-14-5573-2022, 2022.

Champreux, A., Saltré, F., Traylor, W., Hickler, T., and Bradshaw, C.: How to map biomes: quantitative comparison and review of biome-mapping methods, Ecol. Monogr., https://doi.org/10.1002/ecm.1615, 2024.

Clements, F. E.: The development and structure of biotic communities, J. Ecol., 1917.

Conrad, O., Bechtel, B., Bock, M., Dietrich, H., Fischer, E., Gerlitz, L., Wehberg, J., Wichmann, V., and Böhner, J. (2015): System for Automated Geoscientific Analyses (SAGA) v. 2.1.4. Geoscientific Model Development, 8, 1991–2007. doi:10.5194/gmd-8-1991-2015

https://doi.org/10.5194/egusphere-2026-4919
Preprint. Discussion started: 17 September 2026

Cooper, J. P.: Photosynthesis and Productivity in Different Environments, Cambridge University Press, Cambridge, UK, 1975.
Cui, E., Bian, C., Luo, Y., Niu, S., Wang, Y., and Xia, J.: Spatial variations in terrestrial net ecosystem productivity and its local indicators, Biogeosciences, 17, 6237–6246, https://doi.org/10.5194/bg-17-6237-2020, 2020.
Defries, R. S. and Townshend, J. R. G.: Global land cover characterization from satellite data: from research to operational implementation?, Global Ecol. Biogeogr., 8, 367–379, 1999.
Delcourt, H. R., Delcourt, P. A., and Webb, T.: Dynamic plant ecology: the spectrum of vegetational change in space and time, Quaternary Sci. Rev., 1, 153–175, https://doi.org/10.1016/0277-3791(82)90008-7, 1982.
Dinerstein, E., Olson, D., Joshi, A., Vynne, C., Burgess, N. D., Wikramanayake, E., Hahn, N., Palminteri, S., Hedao, P., Noss, R., Hansen, M., Locke, H., Ellis, E. C., Jones, B., Barber, C. V., Hayes, R., Kormos, C., Martin, V., Crist, E., Kiesecker, J., Blaustein, A., Fandino, B., Poilecot, P., Petracca, L., Gasparinetti, P., Whitten, T., Wolf, C., Kubik, G. J., and Saleem, M.: An ecoregion-based approach to protecting half the terrestrial realm, BioScience, 67, 534–545, https://doi.org/10.1093/biosci/bix014, 2017.
Ding, W., Ree, R. H., May, M. R., Brun, P., Hagen, O., Karger, D. N., Skeels, A., Pellissier, L., Xing, Y., and Zimmermann, N. E.: The asynchronous rise of Northern Hemisphere alpine floras reveals general responses of biotic assembly to orogeny and climate change, Sci. Adv., 11, eadz1888, https://doi.org/10.1126/sciadv.adz1888, 2025.
Fischer, C. and Traub, B.: Swiss National Forest Inventory – Methods and Models of the Fourth Assessment, Springer, https://doi.org/10.1007/978-3-030-19293-8, 2019.
Fischer, J.-C., Walentowitz, A., and Beierkuhnlein, C.: The biome inventory – standardizing global biogeographical land units, Global Ecol. Biogeogr., 31, 2172–2183, https://doi.org/10.1111/geb.13574, 2022.
Fisher, R. A., Muszala, S., Verteinstein, M., Lawrence, P., Xu, C., McDowell, N. G., Knox, R. G., Koven, C., Holm, J., Rogers, B. M., Spessa, A., Lawrence, D., and Bonan, G.: Taking off the training wheels: the properties of a dynamic vegetation model without climate envelopes, CLM4.5(ED), Geosci. Model Dev., 8, 3593–3619, https://doi.org/10.5194/gmd-8-3593-2015, 2015.
Gagnon, E., Ringelberg, J. J., Bruneau, A., Lewis, G. P., and Hughes, C. E.: Global Succulent Biome phylogenetic conservatism across the pantropical Caesalpinia Group (Leguminosae), New Phytol., 222, 1994–2008, https://doi.org/10.1111/nph.15633, 2019.
GBIF: The Global Biodiversity Information Facility: What is GBIF?, https://www.gbif.org/what-is-gbif (last access: 2026), 2026.
Gehrig-Fasel, J., Guisan, A., and Zimmermann, N. E.: Tree line shifts in the Swiss Alps: climate change or land abandonment?, J. Veg. Sci., 18, 571–582, https://doi.org/10.1111/j.1654-1103.2007.tb02571.x, 2007.
Gerber, S., Joos, F., and Prentice, I. C.: Sensitivity of a dynamic global vegetation model to climate and atmospheric CO_2, Glob. Change Biol., 10, 1223–1239, https://doi.org/10.1111/j.1529-8817.2003.00807.x, 2004.
Gibson, A. C.: Structure-Function Relations of Warm Desert Plants, Springer Science & Business Media, Berlin, Heidelberg, Germany, 2012.
Gonzalez, P., Neilson, R. P., Lenihan, J. M., and Drapek, R. J.: Global patterns in the vulnerability of ecosystems to vegetation shifts due to climate change, Global Ecol. Biogeogr., 19, 755–768, https://doi.org/10.1111/j.1466-8238.2010.00558.x, 2010.
Grace, O. M.: Succulent plant diversity as natural capital, Plants People Planet, 1, 336–345, https://doi.org/10.1002/ppp3.25, 2019.
Grimm, V. and Railsback, S. F.: Pattern-oriented modeling: a "multi-scope" for predictive systems ecology, Philos. T. R. Soc. B, 367, 298–310, https://doi.org/10.1098/rstb.2011.0180, 2012.
Grisebach, A. H. R.: Die Vegetation der Erde nach ihrer klimatischen Anordnung: ein Abriss der vergleichenden Geographie der Pflanzen, Nature, 5, 458–459, https://doi.org/10.1038/005458a0, 1872.
Grossiord, C., Buckley, T. N., Cernusak, L. A., Novick, K. A., Poulter, B., Siegwolf, R. T. W., Sperry, J. S., and McDowell, N. G.: Plant responses to rising vapor pressure deficit, New Phytol., 226, 1550–1566, https://doi.org/10.1111/nph.16485, 2020.
Hagen, O., Flück, B., Fopp, F., Cabral, J. S., Hartig, F., Pontarp, M., Rangel, T. F., and Pellissier, L.: gen3sis: a general engine for eco-evolutionary simulations of the processes that shape Earth's biodiversity, PLoS Biol., 19, e3001340, https://doi.org/10.1371/journal.pbio.3001340, 2021.
Hallgren, W. S. and Pitman, A. J.: The uncertainty in simulations by a Global Biome Model (BIOME3) to alternative parameter values, Glob. Change Biol., 6, 483–495, https://doi.org/10.1046/j.1365-2486.2000.00325.x, 2000.

https://doi.org/10.5194/egusphere-2026-4919
Preprint. Discussion started: 17 September 2026

Harrison, S. P. and Prentice, I. C.: Climate and CO_2 controls on global vegetation distribution at the last glacial maximum: analysis based on palaeovegetation data, biome modeling and palaeoclimate simulations, Glob. Change Biol., 9, 983–1004, https://doi.org/10.1046/j.1365-2486.2003.00640.x, 2003.
Harrison, S. P., Prentice, I. C., Barboni, D., Kohfeld, K. E., Ni, J., and Sutra, J.-P.: Ecophysiological and bioclimatic foundations for a global plant functional classification, J. Veg. Sci., 21, 300–317, https://doi.org/10.1111/j.1654-1103.2009.01144.x, 2010.
Haxeltine, A. and Prentice, I. C.: BIOME3: an equilibrium terrestrial biosphere model based on ecophysiological constraints, resource availability, and competition among plant functional types, Global Biogeochem. Cy., 10, 693–709, https://doi.org/10.1029/96GB02344, 1996.
Hernández-Hernández, T., Brown, J. W., Schlumpberger, B. O., Eguiarte, L. E., and Magallón, S.: Beyond aridification: multiple explanations for the elevated diversification of cacti in the New World Succulent Biome, New Phytol., 202, 1382–1397, https://doi.org/10.1111/nph.12752, 2014.
Holt, B. G., Lessard, J.-P., Borregaard, M. K., Fritz, S. A., Araújo, M. B., Dimitrov, D., Fabre, P.-H., Graham, C. H., Graves, G. R., Jønsson, K. A., Nogués-Bravo, D., Wang, Z., Whittaker, R. J., Fjeldså, J., and Rahbek, C.: An update of Wallace's zoogeographic regions of the world, Science, 339, 74–78, https://doi.org/10.1126/science.1228282, 2013.
Hordijk, I., Poorter, L., Liang, J., et al.: Effect of climate on traits of dominant and rare tree species in the world's forests, Nat. Commun., 16, 4773, https://doi.org/10.1038/s41467-025-59754-7, 2025.
Humboldt, A. von: Ideen zu einer Physiognomik der Gewächse, in: Views of Nature, 1806.
Joswig, J. S., Wirth, C., Schuman, M. C., et al.: Climatic and soil factors explain the two-dimensional spectrum of global plant trait variation, Nat. Ecol. Evol., 6, 36–50, https://doi.org/10.1038/s41559-021-01616-8, 2022.
Kaplan, J. O.: Geophysical Applications of Vegetation Modeling, Ph.D. thesis, Lund University, Lund, Sweden, https://doi.org/10.5281/zenodo.1492908, 2001.
Kaplan, J. O.: BIOME4: BIOME4 public release (1999) (v4.2.3), Zenodo [code], https://doi.org/10.5281/zenodo.11270258, 2024.
Kaplan, J. O., Bigelow, N. H., Prentice, I. C., Harrison, S. P., Bartlein, P. J., Christensen, T. R., Cramer, W., Matveyeva, N. V., McGuire, A. D., Murray, D. F., Razzhivin, V. Y., Smith, B., Walker, D. A., Anderson, P. M., Andreev, A. A., Brubaker, L. B., Edwards, M. E., and Lozhkin, A. V.: Climate change and Arctic ecosystems: 2. Modeling, paleodata-model comparisons, and future projections, J. Geophys. Res.-Atmos., 108, D19, https://doi.org/10.1029/2002JD002559, 2003.
Keppel, G., Van Niel, K. P., Wardell-Johnson, G. W., Yates, C. J., Byrne, M., Mucina, L., Schut, A. G. T., Hopper, S. D., and Franklin, S. E.: Refugia: identifying and understanding safe havens for biodiversity under climate change, Global Ecol. Biogeogr., 21, 393–404, https://doi.org/10.1111/j.1466-8238.2011.00686.x, 2012.
Klinges, D. H., Maclean, I. M., and Scheffers, B. R.: Redrawing Köppen-Geiger classes with microclimate: implications for nature and society, Front. Ecol. Environ., e2831, https://doi.org/10.1002/fee.2831, 2025.
Kobayashi, T., Tateishi, R., Alsaaideh, B., Sharma, R., Wakaizumi, T., Miyamoto, D., Bai, X., Long, B., Gegentana, G., Maitiniyazi, A., Cahyana, D., Haireti, A., Morifuji, Y., Abake, G., Pratama, R., Zhang, N., Alifu, Z., Shirahata, T., Mi, L., and Phong, D.: Production of global land cover data – GLCNMO2013, J. Geogr. Geol., 9, p1, https://doi.org/10.5539/jgg.v9n3p1, 2017.
Koen, E. L., Bowman, J., Sadowski, C., and Walpole, A. A.: Landscape connectivity for wildlife: development and validation of multispecies linkage maps, Methods Ecol. Evol., 5, 626–633, https://doi.org/10.1111/2041-210X.12197, 2014.
Köppen, W.: Das geographische System der Klimate, in: Handbuch der Klimatologie, edited by: Köppen, W. and Geiger, R., Gebrüder Borntraeger, Berlin, Germany, 1936.
Körner, C. and Paulsen, J.: A world-wide study of high altitude treeline temperatures, J. Biogeogr., 31, 713–732, https://doi.org/10.1111/j.1365-2699.2003.01043.x, 2004.
Kottek, M., Grieser, J., Beck, C., Rudolf, B., and Rubel, F.: World map of the Köppen-Geiger climate classification updated, Meteorol. Z., 15, 259–263, https://doi.org/10.1127/0941-2948/2006/0130, 2006.
Kreft, H. and Jetz, W.: Global patterns and determinants of vascular plant diversity, P. Natl. Acad. Sci. USA, 104, 5925–5930, https://doi.org/10.1073/pnas.0608361104, 2007.
Krinner, G., Viovy, N., de Noblet-Ducoudré, N., Ogée, J., Polcher, J., Friedlingstein, P., Ciais, P., Sitch, S., and Prentice, I. C.: A dynamic global vegetation model for studies of the coupled atmosphere-biosphere system, Global Biogeochem. Cy., 19, GB1015, https://doi.org/10.1029/2003GB002199, 2005.
Lavin, M., Schrire, B. P., Lewis, G., Pennington, R. T., Delgado-Salinas, A., Thulin, M., Hughes, C. E., Matos, A. B., and Wojciechowski, M. F.: Metacommunity process rather than continental tectonic history better explains

https://doi.org/10.5194/egusphere-2026-4919
Preprint. Discussion started: 17 September 2026

geographically structured phylogenies in legumes, Philos. T. R. Soc. B, 359, 1509–1522, https://doi.org/10.1098/rstb.2004.1536, 2004.

Lawrence, D. M., Fisher, R. A., Koven, C. D., Oleson, K. W., Swenson, S. C., Bonan, G., Collier, N., Ghimire, B., Van Kampenhout, L., Kennedy, D., Kluzek, E., Lawrence, P. J., Li, F., Li, H., Lombardozzi, D., Riley, W. J., Sacks, W. J., Shi, M., Vertenstein, M., and Zeng, X.: The Community Land Model version 5: description of new features, benchmarking, and impact of forcing uncertainty, J. Adv. Model. Earth Sy., 11, 4245–4287, https://doi.org/10.1029/2018MS001583, 2019.

Lechartre, C. M. S., Boussange, V., Karger, D. N., Kaplan, J. O., Brun, P., and Zimmermann, N.: Biome.jl v0.1.0: a modular platform for mechanistic biome modeling and hypothesis testing, Zenodo [code], https://doi.org/10.5281/zenodo.21921098, 2026a.

Lechartre, C. M. S., Boussange, V., Karger, D. N., Kaplan, J. O., Brun, P., and Zimmermann, N.: biomeR-v0.0.1: The R API of the Biome.jl package, Zenodo [code], https://doi.org/10.5281/zenodo.22658759, 2026b.

Li, S., Zhang, X., Lu, Z., Ni, J., and Lu, J.: Progress of vegetation modeling and future research prospects, Sci. China Earth Sci., https://doi.org/10.1007/s11430-023-1367-1, 2024.

Loarie, S. R., Duffy, P. B., Hamilton, H., Asner, G. P., Field, C. B., and Ackerly, D. D.: The velocity of climate change, Nature, 462, 1052–1055, https://doi.org/10.1038/nature08649, 2009.

Ma, H., Crowther, T. W., Mo, L., Maynard, D. S., Renner, S. S., van den Hoogen, J., Zou, Y., Liang, J., de-Miguel, S., Nabuurs, G.-J., Reich, P. B., Niinemets, Ü., Abegg, M., Adou Yao, Y. C., Alberti, G., Almeyda Zambrano, A. M., Alvarado, B. V., Alvarez-Dávila, E., Alvarez-Loayza, P., and Zohner, C. M.: The global biogeography of tree leaf form and habit, Nat. Plants, 9, 1795–1809, https://doi.org/10.1038/s41477-023-01543-5, 2023.

Ma, L., Hurtt, G., Ott, L., Sahajpal, R., Fisk, J., Lamb, R., Tang, H., Flanagan, S., Chini, L., Chatterjee, A., and Sullivan, J.: Global evaluation of the Ecosystem Demography model (ED v3.0), Geosci. Model Dev., 15, 1971–1994, https://doi.org/10.5194/gmd-15-1971-2022, 2022.

Maiorano, L., Cheddadi, R., Zimmermann, N. E., Pellissier, L., Petitpierre, B., Pottier, J., Laborde, H., Hurdu, B. I., Pearman, P. B., Psomas, A., Singarayer, J. S., Broennimann, O., Vittoz, P., Dubuis, A., Edwards, M. E., Binney, H. A., and Guisan, A.: Building the niche through time: using 13,000 years of data to predict the effects of climate change on three tree species in Europe, Global Ecol. Biogeogr., 22, 302–317, https://doi.org/10.1111/j.1466-8238.2012.00767.x, 2013.

Marti, B., Yakovlev, A., Karger, D. N., Ragettli, S., Zhumabaev, A., Wakil, A. W., and Siegfried, T.: CA-discharge: geo-located discharge time series for mountainous rivers in Central Asia, Sci. Data, 10, 579, https://doi.org/10.1038/s41597-023-02474-8, 2023.

Midgley, G. F. and Bond, W. J.: Future of African terrestrial biodiversity and ecosystems under anthropogenic climate change, Nat. Clim. Change, 5, 823–829, https://doi.org/10.1038/nclimate2753, 2015.

Moncrieff, G. R., Bond, W. J., and Higgins, S. I.: Revising the biome concept for understanding and predicting global change impacts, J. Biogeogr., 43, 863–873, https://doi.org/10.1111/jbi.12701, 2016.

Mucina, L.: Biome: evolution of a crucial ecological and biogeographical concept, New Phytol., 222, 97–114, https://doi.org/10.1111/nph.15609, 2019.

NASA JPL: NASA Shuttle Radar Topography Mission Global 3 arc second, NASA Land Processes Distributed Active Archive Center [data set], https://doi.org/10.5067/MEASURES/SRTM/SRTMGL3.003 (last access: 30 July 2026), 2013.

Navarro, A., Merino, A., García-Ortega, E., and Tapiador, F. J.: Uncertainty maps for model-based global climate classification systems, Sci. Data, 12, 35, https://doi.org/10.1038/s41597-025-04387-0, 2025.

Neilson, R. P.: A model for predicting continental-scale vegetation distribution and water balance, Ecol. Appl., 5, 362–385, https://doi.org/10.2307/1942028, 1995.

Nobis, M. P. and Normand, S.: KISSMig – a simple model for R to account for limited migration in analyses of species distributions, Ecography, 37, 1282–1287, https://doi.org/10.1111/ecog.00930, 2014.

Norby, R. J. and Zak, D. R.: Ecological lessons from free-air CO_2 enrichment (FACE) experiments, Annu. Rev. Ecol. Evol. S., 42, 181–203, https://doi.org/10.1146/annurev-ecolsys-102209-144647, 2011.

Novoa, A., Le Roux, J., Robertson, M., Wilson, J., and Richardson, D.: Introduced and invasive cactus species: a global review, AoB Plants, 7, plu078, https://doi.org/10.1093/aobpla/plu078, 2015.

Ohsawa, M.: Structural comparison of tropical montane rain forests along latitudinal and altitudinal gradients in south and east Asia, Vegetatio, 97, 1–10, https://doi.org/10.1007/BF00033897, 1991.

Olson, D. M., Dinerstein, E., Wikramanayake, E. D., Burgess, N. D., Powell, G. V. N., Underwood, E. C., D'amico, J. A., Itoua, I., Strand, H. E., Morrison, J. C., Loucks, C. J., Allnutt, T. F., Ricketts, T. H., Kura, Y., Lamoreux, J. F., Wettengel, W. W., Hedao, P., and Kassem, K. R.: Terrestrial ecoregions of the world: a new map of life on Earth, BioScience, 51, 933–938, https://doi.org/10.1641/0006-3568(2001)051[0933:TEOTWA]2.0.CO;2, 2001.

https://doi.org/10.5194/egusphere-2026-4919
Preprint. Discussion started: 17 September 2026

Ordonez, A., Riede, F., Normand, S., and Svenning, J.-C.: Towards a novel biosphere in 2300: rapid and extensive global and biome-wide climatic novelty in the Anthropocene, Philos. T. R. Soc. B, 379, 20230022, https://doi.org/10.1098/rstb.2023.0022, 2024.

Pilowsky, J. A., Colwell, R. K., Rahbek, C., and Fordham, D. A.: Process-explicit models reveal the structure and dynamics of biodiversity patterns, Sci. Adv., 8, eabj2271, https://doi.org/10.1126/sciadv.abj2271, 2022.

Poggio, L., de Sousa, L. M., Batjes, N. H., Heuvelink, G. B. M., Kempen, B., Ribeiro, E., and Rossiter, D.: SoilGrids 2.0: producing soil information for the globe with quantified spatial uncertainty, SOIL, 7, 217–240, https://doi.org/10.5194/soil-7-217-2021, 2021.

Portmann, F. T., Siebert, S., and Döll, P.: MIRCA2000 – global monthly irrigated and rainfed crop areas around the year 2000: a new high-resolution data set for agricultural and hydrological modeling, Global Biogeochem. Cy., 24, GB1011, https://doi.org/10.1029/2008GB003435, 2010.

Poulter, B., Ciais, P., Hodson, E., Lischke, H., Maignan, F., Plummer, S., and Zimmermann, N. E.: Plant functional type mapping for earth system models, Geosci. Model Dev., 4, 993–1010, https://doi.org/10.5194/gmd-4-993-2011, 2011.

Prentice, I. C., Cramer, W., Harrison, S. P., Leemans, R., Monserud, R. A., and Solomon, A. M.: A global biome model based on plant physiology and dominance, soil properties and climate, J. Biogeogr., 19, 117–134, https://doi.org/10.2307/2845499, 1992.

Quillet, A., Peng, C., and Garneau, M.: Toward dynamic global vegetation models for simulating vegetation–climate interactions and feedbacks: recent developments, limitations, and future challenges, Environ. Rev., 18, 333–353, https://doi.org/10.1139/A10-016, 2010.

R Core Team: R: A Language and Environment for Statistical Computing, R Foundation for Statistical Computing, Vienna, Austria [code], https://www.R-project.org/, 2025.

Ringelberg, J. J., Zimmermann, N. E., Weeks, A., Lavin, M., and Hughes, C. E.: Biomes as evolutionary arenas: convergence and conservatism in the trans-continental Succulent Biome, Dryad [data set], https://doi.org/10.5061/dryad.08kprr4zs, 2020a.

Ringelberg, J. J., Zimmermann, N. E., Weeks, A., Lavin, M., and Hughes, C. E.: Biomes as evolutionary arenas: convergence and conservatism in the trans-continental succulent biome, Global Ecol. Biogeogr., 29, 1100–1113, https://doi.org/10.1111/geb.13089, 2020b.

Salzmann, U., Haywood, A. M., Lunt, D. J., Valdes, P. J., and Hill, D. J.: A new global biome reconstruction and data-model comparison for the Middle Pliocene, Global Ecol. Biogeogr., 17, 432–447, https://doi.org/10.1111/j.1466-8238.2008.00381.x, 2008.

Schimper, A. F. W.: Pflanzen-Geographie auf physiologischer Grundlage, 2nd edn., 1–1070, Gustav Fischer, Jena, Germany, https://doi.org/10.5962/bhl.title.46243, 1908.

Smith, B., Prentice, I. C., and Sykes, M. T.: Representation of vegetation dynamics in the modeling of terrestrial ecosystems: comparing two contrasting approaches within European climate space, Global Ecol. Biogeogr., 10, 621–637, 2001.

Smith, T. and Huston, M.: A theory of the spatial and temporal dynamics of plant communities, Vegetatio, 83, 49–69, 1989.

Smith, T. M., Shugart, H. H., Woodward, F. I., and Burton, P. J.: Plant functional types, in: Vegetation Dynamics & Global Change, edited by: Solomon, A. M. and Shugart, H. H., Springer US, New York, USA, 272–292, https://doi.org/10.1007/978-1-4615-2816-6_14, 1993.

Smith, B., Wårlind, D., Arneth, A., Hickler, T., Leadley, P., Siltberg, J., and Zaehle, S.: Implications of incorporating N cycling and N limitations on primary production in an individual-based dynamic vegetation model, Biogeosciences, 11, 2027–2054, https://doi.org/10.5194/bg-11-2027-2014, 2014.

Solomon, A. M. and Shugart, H. H. (Eds.): Vegetation Dynamics & Global Change, Springer, New York, USA, 1993.

Thornthwaite, C. W.: The climates of North America: according to a new classification, Geogr. Rev., 21, 633–655, 1931.

Thornthwaite, C. W.: An approach toward a rational classification of climate, Geogr. Rev., 38, 55–94, https://doi.org/10.2307/210739, 1948.

Tree Cover Density 2012 (raster 20 m), Europe, 3-yearly, Mar. 2018: EEA Geospatial Data Catalogue [data set], https://sdi.eea.europa.eu/catalogue/copernicus/api/records/91687ef2-f907-4f84-81f7-c9c81980c306 (last access: 16 January 2026), 2018.

Troll, C. and Paffen, K. H.: Karte der Jahreszeiten-Klimate der Erde, Erdkunde, 18, 5–28, https://doi.org/10.3112/erdkunde.1964.01.02, 1964.

https://doi.org/10.5194/egusphere-2026-4919
Preprint. Discussion started: 17 September 2026

Wanner, H., Beer, J., Bütikofer, J., Crowley, T. J., Cubasch, U., Flückiger, J., Goosse, H., Grosjean, M., Joos, F., Kaplan, J. O., Küttel, M., Müller, S. A., Prentice, I. C., Solomina, O., Stocker, T. F., Tarasov, P., Wagner, M., and Widmann, M.: Mid- to Late Holocene climate change: an overview, Quaternary Sci. Rev., 27, 1791–1828, https://doi.org/10.1016/j.quascirev.2008.06.013, 2008.

Waser, L., Ginzler, C., Psomas, A., Rüetschi, M., and Rehush, N.: Forest Type NFI [data set], National Forest Inventory (NFI), https://doi.org/10.16904/1000001.7, 2025.

Whittaker, R. H.: Vegetation of the Great Smoky Mountains, Ecol. Monogr., 26, 2–80, https://doi.org/10.2307/1943577, 1956.

Whittaker, R. H.: Communities and Ecosystems, Macmillan, New York, USA, 1970.

Willert, D. J. von: Life Strategies of Succulents in Deserts: With Special Reference to the Namib Desert, CUP Archive, Cambridge, UK, 1992.

Willmes, C., Becker, D., Brocks, S., Hütt, C., and Bareth, G.: High resolution Köppen-Geiger classifications of paleoclimate simulations, T. GIS, 21, 57–73, https://doi.org/10.1111/tgis.12187, 2017.

Wissmann, H.: Die Klima- und Vegetationsgebiete Eurasiens: Begleitworte zu einer Karte der Klimagebiete Eurasiens, 81–92, Gesellschaft für Erdkunde, Berlin, Germany, 1939.

Woodward, F. I.: Climate and Plant Distribution, Cambridge University Press, Cambridge, UK, 1987.

Woodward, F. I. and Williams, B. G.: Climate and plant distribution at global and local scales, Vegetatio, 69, 189–197, https://doi.org/10.1007/BF00038700, 1987.

Woodward, F. I., Lomas, M. R., and Kelly, C. K.: Global climate and the distribution of plant biomes, Philos. T. R. Soc. B, 359, 1465–1476, https://doi.org/10.1098/rstb.2004.1525, 2004.

Wüest, R. O., Zimmermann, N. E., Zurell, D., et al.: Macroecology in the age of Big Data – where to go from here?, J. Biogeogr., 47, 1–12, https://doi.org/10.1111/jbi.13633, 2020.

Zilker, F. and Karger, D. N.: CHELSAch-highres-climatologies at high resolution, EnviDat [data set], https://doi.org/10.16904/envidat.689, 2025.